CHAPTER 6

# Surface- and Solution-Based Assembly of Amyloid Fibrils for Biomedical and Nanotechnology Applications

**Sally L. Gras**

Contents



## 1. INTRODUCTION

Nature uses self-assembling polypeptides to build a staggering variety of protein structures. These proteins act as structural supports, as efficient enzymes, and complex machines. They also take part in sophisticated signaling pathways where they direct and control cell metabolism and growth.

Department of Chemical and Biomolecular Engineering and The Bio21 Molecular Science and Biotechnology Institute, The University of Melbourne, Victoria 3010, Australia.

*E-mail address*: sgras@unimelb.edu.au

Advances in Chemical Engineering, Volume 35
ISSN 0065-2377, DOI: 10.1016/S0065-2377(08)00206-8

This theme of self-assembly, where multiple units come together and form an organized structure, is essential to life and assembly processes can be observed across the phylogenetic kingdom from single-cell organisms to much larger and more complex organisms including humans.

As scientists and engineers, natural self-assembly processes represent a tremendous resource, which we can use to create our own miniature materials and devices. Our endeavors are informed by hundreds of years of curiosity-driven research interested in the natural world. Our toolbox is further expanded by modern synthetic chemistry which extends beyond the realm of natural molecules. We can also create artificial environments to control and direct assembly and use computer-based tools and simulations to model and predict self-assembly pathways and their resulting protein structures. Many researchers believe we can use these modern tools to simplify, improve, and refine assembly processes. We have much to do in order to reach this ambitious goal but the next 10 years are likely to be filled with exciting discoveries and advances as self-assembling polypeptide materials move from the laboratory to the clinic or the manufacturing assembly line.

This chapter describes the self-assembly of non-native protein fibers known as amyloid fibrils and the development of these fibrils for potential applications in nanotechnology and biomedicine. It extends an earlier review by the author on a related topic (Gras, 2007). In Section 1, the self-assembly of polypeptides into amyloid fibrils and efforts to control assembly and any subsequent disassembly are discussed. In Section 2, this review focuses on the important role of surfaces and interfaces during and after polypeptide assembly. It examines how different surfaces can influence fibril assembly, how surfaces can be used to direct self-assembly in order to create highly ordered structures, and how different techniques can be used to create aligned and patterned materials on surfaces following self-assembly.

In Section 3, the ever growing range of potential applications for fibrous self-assembled polypeptide materials is discussed including the development of electronic, photonic, or magnetic components for devices, progress toward platforms for enzyme immobilization and sensors, and advances in biocompatible materials. Comparisons are made between amyloid fibrils and other designed self-assembling fibrous structures throughout this chapter in order to illustrate the diversity of this rapidly expanding field and highlight similarities between the different protein structures and their potential applications.

## 2. POLYPEPTIDE SELF-ASSEMBLY

### 2.1. Amyloid fibrils and other fibrous structures

Amyloid fibrils are non-native protein structures that demonstrate a host of desirable properties, making these fibers attractive components for

nanotechnology and biomedicine (Gras, 2007; Hamada et al., 2004; Macphee and Woolfson, 2004; Stevens and George, 2005; Waterhouse and Gerrard, 2004). These fibrils have a comparable size to other nanostructures; they typically span 10–30 nm in width and reach up to several microns in length. Fibrils are also rich in β-sheet secondary structure and share a cross-beta core structure where β-strands are arranged in β-sheets that stack perpendicular to the fiber axis (Pauling and Corey, 1951).

The highly ordered core of amyloid fibrils is thought to be the basis of their great strength (Smith et al., 2006). Fibrils are also resistant to enzymatic digestion (Zurdo et al., 2001) and can be dehydrated without loss of structural integrity (Squires et al., 2006). The regular placement of polypeptides within the core also allows additional pendant groups to be displayed on the surface of the fibril and ordered on a nanoscale (Baldwin et al., 2006; Baxa et al., 2003; Gras et al., 2008; MacPhee and Dobson, 2000b). Further molecules may also be recruited to the fibril surface using standard chemistries such as antibody interactions, receptor–ligand interactions, biotin–streptavidin binding, and gold–thiol interactions.

Amyloid fibrils are commonly known for their association with a range of protein misfolding diseases (Westermark et al., 2005), where proteins loose their native shape and associate through a series of sequential steps eventually adopting a cross-beta structure (Sunde et al., 1997). These fibrils were initially thought to be the cause of disease but it is now generally thought that the protein structures found early on the fibrillation pathway may be responsible for toxicity, with fibrils possibly being inert structures (Bucciantini et al., 2002; Mucke et al. 2000).

Increasingly amyloid fibrils are being discovered in nature where they may demonstrate a positive role, as structures that help bacteria to colonize new surfaces (Chapman et al., 2002), as bacterial extensions that modify surface tension (Claessen et al., 2003; Talbot, 2003), and as structures that aid the polymerization of melanin in our own cells (Fowler et al., 2006). This insight together with the hypothesis that the generic nature of a polypeptide backbone allows all proteins to adopt a highly regular β-sheet structure and form amyloid fibrils (Dobson, 1999; Fandrich et al., 2003; Guijarro et al., 1998) suggests that designed amyloid fibrils could be used as highly functional materials for a wide range of applications.

Amyloid fibrils can be constructed from a range of raw materials including de novo-designed peptides, cheap proteins that are typically found in the laboratory, inexpensive waste proteins (Garvey et al., 2008, Pearce et al., 2007), or proteins that can be produced by recombinant expression in a host cell such as a bacterial or plant cell. Computer models and simulations including phenomenological models and atomistic simulations will certainly play an important role in the design or selection of protein sequences for amyloid fibril formation due to their ability to predict aggregation-prone regions (Caflisch, 2006). Molecular dynamics, coarse-grained models, and Monte Carlo

simulations are also valuable for their ability to model the behavior of monomers and the assembled structures (Colombo et al., 2007). An understanding of the energetic parameters involved in self-assembly can also be used to produce structures with different morphologies such as tapes and ribbons, and this understanding can be applied to promote gel formation (Aggeli et al., 1997).

Other self-assembling polypeptide systems form nanofibrous structures that resemble the appearance of amyloid fibrils by microscopy. These include but are not limited to diphenylalanine nanofibers (Reches and Gazit, 2003), peptide amphiphiles (Hartgerink et al., 2001), and ionic complementary self-assembling peptides (Holmes et al. 2000). These systems can be rich in β-sheet secondary protein structure but often differ in their self-assembly pathways, the forces driving assembly, and the final arrangement of polypeptides within the resulting fiber. The term "fiber" is used within this chapter to refer to these structures and distinguish from amyloid "fibrils" that have a cross-beta structure.

The Phe–Phe motif used to form diphenylalanine peptide nanotubes was originally derived from the hydrophobic portion of the Aβ peptide which forms amyloid fibrils associated with Alzheimer disease (Reches and Gazit, 2003). This motif was found to be sufficient to drive assembly of peptide nanotubes, which are hollow and thought to be stabilized by ring stacking (Reches and Gazit, 2003). The peptide amphiphiles developed by Stupp and other researches consist of a hydrophobic alkyl tail and a β-sheet-forming hydrophilic peptide which assembles into a cylindrical fiber with the hydrophilic peptide facing the solvent (Hartgerink et al., 2001). Ionic complementary self-assembling peptides also have an amphiphilic nature. They consist of alternating hydrophilic and hydrophobic residues, where the hydrophilic group has alternating positive and negative charges, providing ionic complementary (Hong et al., 2003). These motifs were originally isolated from a yeast Z-DNA-binding protein (Zhang et al., 1993). Each of these systems has great potential as structures for nanotechnology and biomedicine.

This chapter focuses on amyloid fibrils formed by polypeptides and contrasts developments in our understanding of fibril assembly with developments reported for the other selected self-assembling systems described above. Amyloid fibrils can be formed from protein–polymer hybrids (Channon and Macphee, 2008), and there is further scope to create fibrillar structures that incorporate lipids (Griffin et al., 2008) or carbohydrates (Alexandrescu, 2005). The range of possible self-assembling polypeptide sequences and structures is much wider than can be included within this chapter and the reader is directed to other studies describing structures built from cyclic peptides (Ghadiri et al., 1993), structures from helical proteins (Woolfson and Ryadnov, 2006) and the broad principles for the design of other self-assembling polypeptide systems (Bromley et al., 2008).

## 2.2. Amyloid fibril assembly, stability, and disassembly

If amyloid fibrils and other self-assembling polypeptide systems are to be developed as new materials and components for nanotechnology and biomedicine, it is important that we understand the pathways and kinetics of their assembly. It will also be desirable to be able to control this assembly and any subsequent disassembly.

Amyloid fibrils are highly stable once fully formed and can withstand extreme conditions including pressures as high as 1.3 GPa (Meersman and Dobson, 2006). However, there is increasing evidence that amyloid fibrils are dynamic structures that are in exchange with monomeric peptides in solution (Carulla et al., 2005). Assembly is also reversible under some conditions such as changes in pH, the addition of solvents, or use of antibodies or denaturants (MacPhee and Dobson, 2000a; Meersman and Dobson, 2006). While stability will be important for many functions and could be enhanced by cross-linking, disassembly may also prove useful for materials designed for temporary use or materials designed to release associated drugs, biomolecules, or other cargo into the surrounding environment.

A number of techniques can be used to monitor the growth of amyloid fibrils and provide information on the kinetics of fibril assembly or disassembly. These techniques include light scattering or dye binding assays where Thioflavin T binds to the emerging fibril structure resulting in an increase in fluorescence (Krebs et al., 2005). Fourier transform infrared spectroscopy and circular dichroism can be used to monitor a change in secondary structure as the polypeptide adopts a β-sheet-rich confirmation (Nilsson, 2004) and a quartz crystal oscillator used to follow an increase in fibril mass as a function of time (Knowles et al., 2007).

Complementary microscopy techniques can be used to follow the morphology and growth of fibrils either on a surface or in aliquots taken from the assembly solution including total internal reflection fluorescence microscopy (TIRFM) (Ban et al., 2004), transmission electron microscopy (TEM), or atomic force microscopy (AFM).

Fibril formation is a nucleated process that is characterized by an initial lag phase (Devlin et al., 2006; Hortschansky et al., 2005). Nucleation is followed by a fibril growth phase known as elongation. The assembly kinetics then plateau as the majority of polypeptide is incorporated into fibrillar structures. The final portion of polypeptide incorporated into fibrils is characteristic to a particular fibril system and can vary from low conversions to greater than 99% of all protein in the sample (Gras et al., 2008).

Seeding is one way of potentially controlling what is typically an uncontrolled fibril assembly process, where polypeptide building blocks are combined in solution under favorable conditions. Seeds are short fibril fragments that can nucleate fibril growth, eliminate the lag phase, and

accelerate assembly. To be successful, seeding requires a high sequence identity between the sequence used to construct the seeds and the sequence of polypeptide which is being seeded (Krebs et al., 2004; Wright et al., 2005). This specificity has the added advantage of promoting the growth of a single fibril type from a solution containing multiple proteins, potentially allowing fibril growth from unpurified protein mixtures.

The conditions used to initiate fibril growth can also be used to control assembly. Parameters such as solution temperature, pH, and the ionic concentration are all known to influence the efficiency of the assembly process and can be used to exert control. For example, unfavorable low temperatures could be used to store polypeptide building blocks in order to prevent assembly. The temperature can then be raised to induce assembly. The designed "ccbeta switch system" behaves in this manner; changing from a coiled coil structure to an amyloid fibril when the temperature is increased (Kammerer and Steinmetz, 2006). The challenge with this approach is to design polypeptides so that they effectively respond to stimuli that are compatible with proposed applications. Agelli and colleagues (2003) have effectively illustrated this approach, rationally introducing Glu and Orn side chains so that peptide assembly is responsive to pH.

Other stimuli successfully used for temporal control of fibril assembly include chemical or enzymatic switches and light, often involving an O—N intramolecular acyl migration which increases peptide solubility (Sohma et al., 2004). Dos Santos used O—N intramolecular acyl migration to switch the Aβ peptide from a stable monomer to an assembly competent state (Dos Santos et al., 2005). Switch elements consisting of an ester and a flexible C—C bond were placed along the backbone increasing monomer stability. These residues were then removed using proteases, triggering O—N intramolecular acyl migration and fibril assembly. Other stimuli used by Dos Santos to induce O—N intramolecular acyl migration and assembly included pH and light. Similarly, Taniguchi and colleagues explored a phototriggered click reaction followed by O—N intramolecular acyl migration to generate an analog of Aβ1-42 (Taniguchi et al., 2006). Whereas Bosques used a photoliable linker to initiate fibril assembly (Bosques and Imperiali, 2003).

Pseudoproline units offer another approach for controlling fibril assembly (Tuchscherer et al., 2007). Serine, threonine, or cystiene residues may be replaced with pseudoproline. The pseudoproline ring introduces a cis–amide bond in the backbone preventing aggregation and increasing peptide solubility. The ring can be cleaved during the final deprotection stage of fluoren-9-ylmethyloxycarbonyl (FMOC) synthesis or by treatment with acid when assembly is desired. Tuchscherer and colleagues also present evidence that the pseudoproline approach may be more effective than incorporating *O*-acyl groups at preventing the stable monomer from forming fibrils (Tuchscherer et al., 2007).

The chemistry used to control fibril assembly may also be applied to influence morphology, structure, disassembly, and the spatial control of fibrils. Switch elements responding to different signals may be placed in distinct sections of a fibril-forming peptide potentially offering a programmable way to change fibril structure and morphology (Tuchscherer et al., 2007). O—N intramolecular acyl migration can also be used to trigger the transition from a β-sheet confirmation to an α-helical structure disrupting preformed amyloid fibrils (Mimna et al., 2007). A strategy of UV-cleavable linkers applied to disassemble peptide amphiphiles by Lowik and colleagues (2008) may also be applied to fibrils. Lowick suggests these linkers may prove useful for controlling the placement of fibers on a surface, where a UV source and mask may be used to spatially control patterned areas of assembled and disassembled fibers.

## 3. THE ROLE OF SURFACES DURING AND AFTER ASSEMBLY

Surfaces and interfaces play an important role in the formation of fibrous structures from polypeptides. While the majority of assembly processes are conducted in solution within a bulk liquid phase, this liquid will be bounded by a single interface or combination of interfaces including solid–liquid interfaces, liquid–liquid interfaces, or liquid–gas interfaces each which can influence the assembly process, as illustrated in Figure 1.

An understanding of the interaction between polypeptides and surfaces is imperative if self-assembly is to be achieved in a reproducible manner. This is especially important if the scale of assembly is to be increased from small-scale laboratory experiments to larger reaction vessels. Insights obtained into surface-based assembly can also be used to design surface-based "reactor platforms" which encourage surface interactions in order to achieve

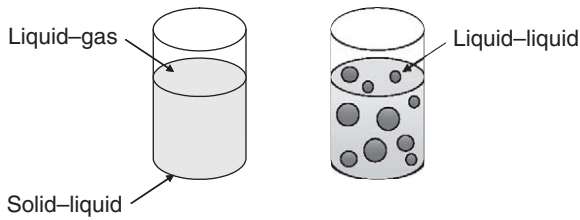


**Figure 1** Interfaces that can be present during the self-assembly of polypeptides in the bulk liquid phase. The left image depicts a common experimental procedure where structures are assembled in a solution contained by a small tube, exposing polypeptides to both solid–liquid and liquid–gas interfaces. A third possible interface is a liquid–liquid interface depicted in the image on the right that contains a solution of two immiscible liquids.

controlled assembly (Nielsen et al., 2001). In Section 3.1 below, the assembly of amyloid fibrils in the presence of surfaces is discussed, with emphasis on the influence of solid nonbiological surfaces. The placement of nanofibers will be critical to many potential applications for fibrils and the use of surfaces to direct fibril assembly and produce patterned materials is subsequently reviewed in Section 3.2.

Surfaces and interfaces remain an important consideration following self-assembly. Fibrous proteins may be specifically designed to interact with surfaces as part of devices either by adsorption or by covalent attachment to the surface. They can also be used to coat surfaces, changing their properties. Our ability to precisely place these fibrils on a surface will determine the range of potential uses for these materials. Interfacial contact can also occur during storage, for example, fibrils in liquid solutions that are stored in plastic containers will encounter both a liquid–polymeric interface and a liquid–air interface. Studies examining the interaction of preassembled fibrils with solid nonbiological surfaces are therefore reviewed in Section 3.3.

## 3.1. Surface-based assembly

A surface or interface can influence the assembly of fibrils by altering both the process and kinetics of fibril nucleation or elongation. This behavior is not surprising as surface properties are known to influence the absorption, confirmation, and destabilization of globular proteins or smaller peptides (Rocha et al., 2005). Surface properties influence fibril assembly in a similar way by altering the absorption, unfolding, and aggregation of monomers.

Key surface properties that can influence fibril assembly include hydrophobicity or hydrophilicity, the presence of negative or positive charges, and surface roughness. Two methods which can be used to characterize surface properties and rationalize interactions between proteins and surfaces are surface wettability and the root mean squared (RMS) roughness. Surface wettability is measured via the contact angle formed when a droplet of water is placed on a surface. A small contact angle indicates a highly wetting surface. The RMS can be measured using an AFM and reflects the variation in surface height about an average surface height. A high RMS indicates a rough surface. Techniques such as streaming potential and AFM can also be used to measure surface charge (Franks and Meagher, 2003) and further characterize a surface.

A number of studies have examined fibril formation in the presence of different solid nonbiological surfaces, as summarized in Table 1. While many of these studies have focused on the formation of fibrils, the wettability and RMS of some surfaces have been characterized. Typical surface contact angles are also presented in Table 1 to aid comparison between these surface-based experiments.

**Table 1** Examples of surface-induced nucleation and growth of fibrils

| Surface | Properties | Polypeptide | Fibril formation | Reference |
|---|---|---|---|---|
| Regenerated cellulose (RE) | Contact angle 27° ± 2, RMS ~ 87 nm | Human insulin | Nucleation faster than bulk | Nayak et al. (2008) |
| Poly(ethersulfone) (PES) | Contact angle 55° ± 2, RMS ~ 36 nm. | Human insulin | Nucleation faster than bulk | Nayak et al. (2008) |
| Poly(vinylidine difluoride (PVDF) | Contact angle 76° ± 2, RMS ~ 195 nm | Human insulin | Nucleation faster than bulk. Elongation not different to the bulk | Nayak et al. (2008) |
| Polyethylene (PE) | Contact angle 94° ± 4, RMS ~ 45 nm | Human insulin | Nucleation faster than bulk. Elongation not different to the bulk | Nayak et al. (2008) |
| Polytetrafluoroethylene (PTFE) | Contact angle 120° ± 3, RMS ~ 54 nm | Human insulin | Nucleation faster than bulk. Elongation not different to the bulk | Nayak et al. (2008) |
| *N*-isopropylacrylamide-co-*N*-tert-butylacrylamide (NIPAM/BAM) copolymer particles (polymer ratio 85:15) | Contact angle ~53° for equivalent flat film | Human $\beta_2$-microglobulin | Nucleation faster than bulk. Elongation not different to the bulk | Allen et al. (2003); Linse et al. (2007) |

**Table 1** (*Continued*)

| Surface | Properties | Polypeptide | Fibril formation | Reference |
|---|---|---|---|---|
| NIPAM/BAM copolymer particles (polymer ratio 50:50) | Contact angle ~57° for equivalent flat film | Human $\beta_2$-microglobulin | Nucleation faster than bulk. Elongation not different to the bulk | Allen et al. (2003); Linse et al. (2007) |
| Hydrophilic polymer-coated quantum dots, cerium oxide particles, and multiwalled carbon nanotubes | – | Human $\beta_2$-microglobulin | Nucleation faster than bulk. Elongation not different to the bulk | Linse et al. (2007) |
| Polystyrene (PS) | Contact angle ~90°[a] | Bovine insulin | Nucleation faster than bulk. Elongation slower than the bulk | Smith et al. (2007); Narrainen et al. (2006) |
| Mica unmodified | Hydrophilic and negatively charged Contact angle <10°[b] | Light chain variable domain from light chain amyloidosis (SAM) | Growth observed but not divided into nucleation and elongation phases | Zhu et al. (2002); Yang et al. (2007) |
| Mica modified | Hydrophilic and positively charged | Light chain variable domain from light chain amyloidosis (SAM) | No growth observed | Zhu et al. (2002) |

| | | | | |
|---|---|---|---|---|
| Mica modified | Hydrophobic | Light chain variable domain from light chain amyloidosis (SAM) | No growth observed | Zhu et al. (2002) |
| Highly oriented pyrolitic graphite (HOPG), ZYB grade | Hydrophobic Contact angle ~71°[c] | Aβ1-42 | Growth observed but not divided into nucleation and elongation phases | Kowalewski and Holtzman, (1999); Yang et al. (2007) |
| Mica unmodified | Hydrophilic and negatively charged Contact angle <10°[b] | Aβ1-42 | Growth observed but not divided into nucleation and elongation phases | Kowalewski and Holtzman, (1999); Yang et al. (2007) |
| Highly oriented pyrolitic graphite (HOPG), ZYH grade | Hydrophobic basal planes and hydrophilic step edges Contact angle ~71°[c] | Aβ1-40, Aβ1-42, and Aβ1-28. | Nucleation observed on hydrophobic surface and growth on hydrophilic surface for both Aβ1-40 and Aβ1-42. No growth observed for Aβ1-28 | Losic et al. (2006); Yang et al. (2007) |

**Table 1** (*Continued*)

| Surface | Properties | Polypeptide | Fibril formation | Reference |
|---|---|---|---|---|
| Mica unmodified | Hydrophilic and negatively charged Contact angle <10°[b] | Aβ1-40 | No growth observed | Losic et al. (2006); Yang et al. (2007) |
| Mica unmodified | Hydrophilic and negatively charged Contact angle <10°[b] | Recombinant $\beta_2$-microglobulin | No growth observed | Relini et al. (2006); Yang et al. (2007) |
| Mica modified | Positively charged | Recombinant $\beta_2$-microglobulin | Fibril growth observed | Relini et al. (2006) |

[a] Typical contact angle for a polystyrene film.

[b] Typical contact angle for freshly cleaved mica.

[c] Typical contact angle for HOPG.

It is clear that a solid surface can nucleate fibril formation under conditions where fibrils are not observed in a bulk liquid phase (Zhu et al., 2002). The surface may act to increase the local concentration of protein and alter the conformation of those proteins leading to an increased propensity for association (Linse et al., 2007; Nayak et al., 2008). However, not all surfaces are equal in their ability to nucleate fibrils, and differences are reported in the literature. One of the most systematic and quantitative studies in fibril nucleation was performed using a range of synthetic surfaces suspended in a bulk solution during the formation of insulin fibrils (Nayak et al., 2008). Nayak and colleagues found that fibril nucleation was accelerated on all surfaces relative to nucleation in a bulk solution and was fastest on rough hydrophobic surfaces. A near-linear inverse correlation was observed between both hydrophobicity or roughness and the lag phase and fibril growth. Similar results were reported by Smith who observed faster nucleation of insulin on a hydrophobic polystyrene surface compared to nucleation in the bulk phase (Smith et al., 2007).

A range of nanoparticles (copolymer particles, quantum dots, cerium oxide particles, and carbon nanotubes) with high surface area have also been shown to accelerate fibril growth relative to fibril growth in solutions lacking nanoparticles (Linse et al., 2007). Specifically, an increase in the surface area of polymeric nanoparticles decreased the lag phase of fibril growth. However, in contrast to Nayak's findings, Linse observed that small increases in copolymer hydrophobicity ($\sim$4°, Table 1) delayed nucleation. Surface plasmon resonance was also used to show that protein binding to hydrophobic particles was weaker than protein binding to hydrophilic particles. Zhu similarly found that hydrophobic surfaces failed to stimulate the nucleation and growth of SAM fibrils (Zhu et al., 2002).

The difference between the findings of Nayak and those of Linse and Zhu could be due to the curved particle surface in the nanoparticle study (Nayak et al., 2008) or differences in surface roughness. These findings also indicate that the protein under consideration, insulin in the case of Nayak's study and $\beta_2$-microglobulin or SAM within Linse and Zhu's studies, may experience different surface interactions. It is certainly likely that the protein hydrophobicity, charge, structure, and size will all influence surface interactions, suggesting that a wide ranging investigation on the effect of surface-induced nucleation for different proteins is required.

Fibrils have been observed to grow on both hydrophobic and hydrophilic surfaces (Kowalewski and Holtzman, 1999). However, the effect of surface hydrophobicity on fibril elongation and growth appears unclear. Smith found fibril growth on polystyrene was slower than in the bulk phase (Smith et al., 2007) and suggested that growth on a polystyrene surface results in different associations between the proteins compared to growth in the bulk phase. However, the growth kinetics observed by Linse in the presence of various nanoparticles (Linse et al., 2007) and by Nayak in the

presence of various polymeric surfaces did not appear significantly altered by the presence of these surfaces in these later studies (Nayak et al., 2008). Growth rates were also similar across different surface types. Interestingly, when both hydrophilic and hydrophobic surfaces are presented in the solution at the same time, as can occur for particular grades of highly ordered pyrolytic graphite (HOPG), Aβ1-40 fibrils grow on the hydrophilic surface (Losic et al., 2006). Losic suggests that nucleation may initiate on the hydrophobic surface.

Electrostatic charges on surfaces can also influence fibril nucleation and growth. The light chain variable domain from light chain amyloidosis (SAM) was found to form fibrils on negatively charged hydrophilic mica but not on positively charged mica (Zhu et al., 2002). Conversely, $\beta_2$-microglobulin forms fibrils on positively charged mica but not on negatively charged mica (Relini et al., 2006). Relini and colleagues observed a decrease in the charge of $\beta_2$-microglobulin during incubation and suggest that the positively charged surface helps dipole crowding and alignment when the protein comes in contact with the surface. These examples highlight the importance of electrostatics in determining which surfaces will support fibril growth. If we are to predict such interactions, we must also consider the charges on a protein and the distribution of these charges throughout a protein, as such charges will be placed in different parts of the protein and will change as a function of pH due to the ionization of protein side chains. The distribution and exposure of hydrophobic regions that are likely to mediate interactions with a hydrophobic surface will also vary within a protein.

There is certainly evidence that protein properties, including the propensity for fibril formation, influence fibril nucleation and growth on a surface. For example, the peptides Aβ1-40, Aβ1-42, and Aβ1-28 behave differently reflecting their different propensities to form fibrils (Losic et al., 2006). Aβ1-42 forms fibrils most readily, and Aβ1-42 fibrils are observed on both mica and HOPG (Kowalewski and Holtzman, 1999; Losic et al., 2006). In contrast, Aβ1-40 forms fibrils on HPOG but not mica, and Aβ1-28, the least prone to aggregation, forms fibrils on neither surface (Losic et al., 2006).

One technique which can be used to systematically examine the effect of surface properties on amyloid fibril growth is high-resolution AFM or kymography. This technique has recently been used to scan along the length of the fibril to determine the stepwise rate of fibril elongation from each of the fibril ends (Kellermayer et al., 2008), and it could be used to examine the influence of surface properties on individual fibrils. Ultimately, it will also be desirable to combine observations of fibril morphology on a surface with information about the kinetics of protein unfolding, rearrangement, and fibril assembly. This information would provide insight into the mechanism of fibril formation. It will also help us to direct fibril formation on surfaces where it may be desired and to prevent unwanted aggregation such as on surgical instruments and dialysis membranes (Nayak et al., 2008).

Fibril formation is known to occur at interfaces other than solid–liquid interfaces, such as lipid–water interfaces (Adams et al., 2002; Sharp et al., 2002). At lipid–water interfaces, fibril formation is strongly influenced by surface charge, and aggregation differs to processes in the bulk solution. Biological molecules such as collagen provide further types of interfaces (Relini et al., 2006) which can be used to induce fibril formation. These interactions offer further opportunities for directing the formation of fibrils but are beyond the scope of this chapter. The reader is directed to a recent review (Stefani, 2007) which discusses the role of membranes and biomacromolecules in stimulating fibril formation in greater detail.

## 3.2. Surface-directed assembly

Surfaces can do more than stimulate the growth of amyloid fibrils; the presence of a surface during assembly can also influence fibril morphology. Fibril diameter has been observed to be smaller on surfaces than in the bulk for some polypeptide systems (Zhu et al., 2002). This may be due to the constraints imposed by the surface or could result from a different mechanism of fibril growth. The shape of fibrils formed on surfaces can also differ to the shape of fibrils formed in the bulk solution.

One of the most interesting properties of highly orientated surfaces is their ability to direct fibril orientation, and this order can be used to create networks and patterns of fibrils on the surface. This trait could be used to determine where fibrillar components assemble within devices or to create patterns for nanoelectronic circuits. A number of biomaterials also involve β-sheet lamination on an inorganic surface (Brown et al., 2002). The surface growth of fibrils, known as epitaxial growth or surface templated assembly, relies on the underlying crystallographic symmetry of the surface material and is analogous to the growth of one crystal phase on top of a host crystal (Kowalewski and Holtzman, 1999).

Kowalewski and colleagues found that Aβ1-42 fibrils formed in three major directions on HOPG as shown in Figure 2 (Kowalewski and Holtzman, 1999). Similar growth has been observed by a range of researchers for Aβ fibrils on HPOG (Kellermayer et al., 2008; Losic et al., 2006). These patterns have also been observed for de novo-designed β-sheet-rich nanofibers constructed from alternating polar and nonpolar sequences (Brown et al., 2002) that resemble amyloid fibrils, as shown in Figure 3. This figure illustrates how epitaxial growth is not limited to individual fibers, with thick layers of more than 10 fibers assembling in the same direction.

The orientated growth of Aβ fibrils and peptide nanofibers on HPOG is due to the underlying six-fold symmetry of the graphite surface. This directs fiber formation in the three observed directions, each orientated at 120°, as illustrated in the schematic in Figure 3. Kowalewski suggested such growth is driven by hydrophobic forces (Kowalewski and Holtzman, 1999), where

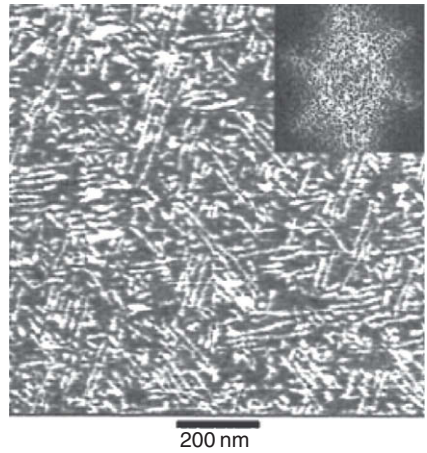


**Figure 2** The orientated growth of Aβ1-42 fibrils from an aqueous solution onto a highly orientated pyrolytic graphite surface. The fibrils are orientated in three directions, each angled at 120°, reflecting the crystalline structure of the underlying material. The image was collected by atomic force microscopy. The inset is a two-dimensional Fourier transform showing the six-fold symmetry of the graphite material (Kowalewski, 1999) (copyright © The National Academy of Sciences of the United States of America, all rights reserved, 1999).

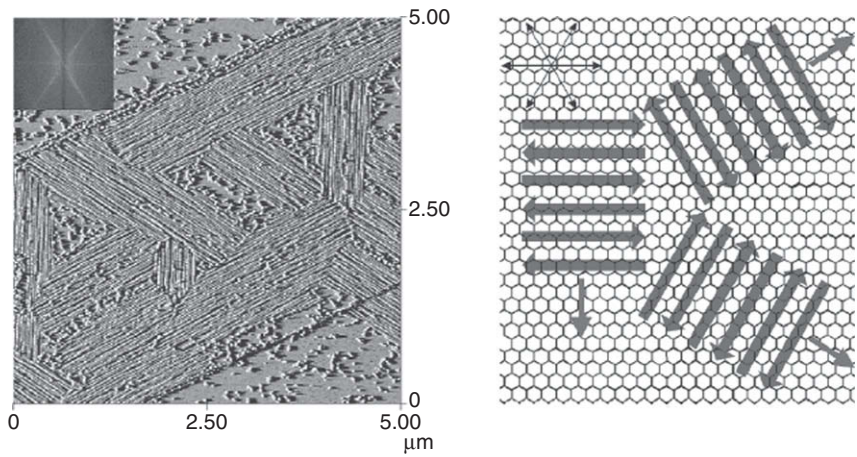


**Figure 3** The orientated growth of peptide fibers formed from an alternating sequence of polar and nonpolar amino acids on a highly orientated pyrolytic graphite surface (left). The image was collected by atomic force microscopy. The inset is a two-dimensional Fourier transform showing the six-fold symmetry of the graphite material. This symmetry is also shown in the schematic (right) which shows how the surface symmetry directs the growth of the fibers, shown as six stranded assemblies, that grow in the direction of the arrow. Reprinted with permission from Brown et al., (2002) (copyright 2002 American Chemical Society).

hydrophobic interactions are maximized by contact between the carbons in graphite and the hydrophobic residues within the peptide chain.

Recently, Losic and colleagues (2006) used steps in HPOG, known as step edges, to direct the growth of Aβ fibrils. Losic specifically choose lower grade graphite with a mosaic angle of $3.5 \pm 1.5°$. This graphite is less ordered than the graphite used by Kowaleski, with a smaller grain size (~30–40 nm rather than 1 μm). The lower grade graphite still contains the regular hydrophobic basal planes containing fused hydrophobic rings, but it also contains more frequent changes in surface height of 0.3–3.6 nm called step edges. These edges are hydrophilic and display a number of functional groups (phenolic, carboxylic, and ketonic groups) (Losic et al., 2006). Losic found that Aβ1-40 and Aβ1-42 fibrils assembled preferentially along the hydrophilic step edges of HPOG rather than on the hydrophobic basal planes as occurs for more ordered graphite. The resulting long straight fibrils are shown in Figure 4.

It is worth noting that not all protein fibers will assemble along the edge of HPOG steps like Aβ fibrils. Yang and colleagues (2007) found that fibers formed from the EAK16-II polypeptide sequence did not form along HPOG edges. Instead these fibers draped over the step edges and their assembly was not influenced by the different chemistry along the edge of the graphite step. The polypeptides that make up these fibers consist of alternating polar and nonpolar residues, resulting in a hydrophilic and hydrophobic face, and this structure is likely to determine the behavior of these fibers on a HOPG surface.

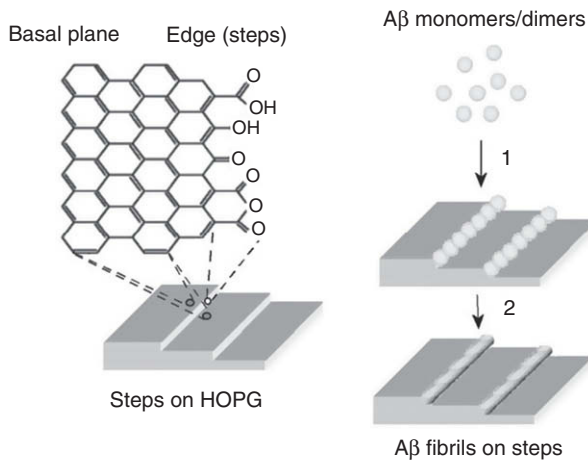


**Figure 4** Schematic illustrating the orientated growth of Aβ1-40 fibrils along the hydrophilic step edges of highly orientated pyrolytic graphite (HOPG) in preference to assembly on the hydrophobic basal plane surface. Copyright (Losic, Martin et al., 2006). Reprinted with permission of John Wiley & Sons, inc.

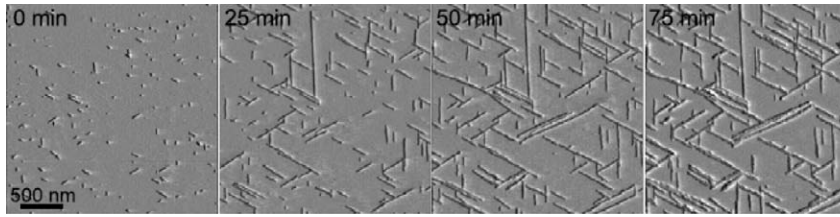


**Figure 5** The orientated growth of Aβ25-35 fibrils from an aqueous solution on a mica surface. The fibrils grow along three main directions, each orientated at 120°. The images were collected by *in situ* time lapse Atomic Force Microscopy (Karsai, Grama et al. 2007). Copyright IOP Publishing Ltd. Reproduced with permission.

The hexagonal crystalline lattice of mica can also be used to direct fibril growth. Karsai and colleagues (2007, 2008) have assembled fibrils from the Aβ25-35 peptide and an N27C cystiene variant on mica. The resulting fibrillar networks are trigonally oriented at 120°, as shown in Figure 5. In contrast, no order is observed for the assembly of the same fibrils formed on a glass surface. Electrostatic attraction appears to govern this type of fibril binding. Specifically, amino groups of lysine residues or the N terminus of the peptide are thought to interact with the potassium binding pockets in mica. The growth of Aβ25-35 is sensitive to potassium ions or amine acetylation, consistent with this proposed mechanism (Karsai et al., 2007). The growth of fibrils from the N27C cystiene variant is also sensitive to sodium chloride (Karsai et al., 2008), and this sensitivity provides a further mechanism for the control of fibril growth.

Surface-based assembly can also be combined with different drying methods to create different surface effects and ordered arrays. Whitehouse and colleagues (2005) studied the ordered assembly of β-sheet tapes on mica and used a blotting method to dry the surface, where excess solution was removed from the side of the surface by wicking with filter paper. The shear forces created by this blotting created highly ordered arrays of fibrils suggesting that this method could be used to generate large aligned monolayers. It should be noted that methods that involve drying such as the blotting technique involve interactions with the liquid–air interface in addition to the solid–liquid interface. The blotting method also has some similarities to molecular combing method outlined in Section 3.3 below. A significant difference, however, is that the blotting method described by Whitehouse involves assembly and alignment rather than the alignment of preformed fibers.

Surface assembly can also be used to orientate fibrils relative to the surface, generating fibrils that are horizontal or perpendicular to a surface. Zhang observed this behavior for the artificial GAV9 peptide which contains the consensus sequences from α-synuclein, Aβ, and the prion protein (Zhang et al., 2006). This peptide assembles horizontally on HOPG surfaces and assembles perpendicular to the surface of mica.

The orientated growth of fibrils is dependent on the properties of both the surface and the polypeptide, similar to nonorientated fibril growth discussed in Section 3.1 above. For example, not all Aβ peptides assemble along the step edges on HPOG (Kellermayer et al., 2008; Losic et al., 2006). Hoyer also found that α-synuclein assembles on mica but not on HOPG (Hoyer et al., 2004), which the authors suggest is due to differences in electrostatic attraction between the two surfaces. Consequently, any insights that can be gained for surface nucleation and growth on nonorientated surfaces will help to advance our understanding for surface-directed assembly. It will also inform attempts to construct artificial surfaces with features designed to direct and exploit such fibrillar assembly.

External microscopy tools can be used to further control the surface-based assembly of fibrils on a surface. Kowalewski used an AFM tip to move the initial aggregates that first form during fibril assembly and change their position on a surface (Kowalewski and Holtzman, 1999). An AFM tip has also been used to induce fibril disassembly in restricted areas (Kellermayer et al., 2008), and both methods offer a way to create patterns of fibrils on a surface.

The growth of fibril ends will be important for creating arrays. In some cases fibril growth is unidirectional; in other cases growth appears to be bidirectional, although the speed of assembly can significantly differ between fibril ends (Inoue et al., 2001; Kellermayer et al., 2008; Scheibel et al., 2001). An interesting feature of fibril growth is that it aborts when the fibril reaches another fibril obscuring its path. When confronted with an obstacle, the fibrils do not change direction or grow over the obstacle; however, an AFM tip can be used to change the direction of fibril growth (Zhang et al., 2006). This behavior could only be induced by Zhang on mica and not on HPOG, possibly due to the different orientation of the fibrils formed by the GAV9 peptide on these surfaces.

One possible drawback of surface-directed assembly is that this phenomenon has been observed to decrease for some fibrils, such as Aβ25-35, as the fibrils reach the later stages of assembly (Karsai et al., 2007). This temporal change could possibly be avoided by using higher concentrations of Aβ25-35 peptide during assembly. Chemical cross-linking could also be used to capture the fibrils on the surface and stabilize the fibril network.

Information on the stability of fibrils will be critical for assessing the potential of fibril-coated surfaces for biotechnology applications. Fibrils such as insulin remain strongly bound to the surface after formation and remain on the surface after rinsing with water (Zhu et al., 2002). This is a desirable feature for the construction of new materials, although there may be some instances where surface transfer is required.

The surface stability of other self-assembling fiber systems such as EAK16-II have been extensively characterized (Yang et al., 2007). These fibers are stable on HOPG under both acidic and basic conditions, most

likely due to the hydrophobic nature of the fiber–surface interaction. In contrast, on mica where electrostatic interactions are likely to dominate these EAK16-II, fibers are stable under acidic conditions but unstable under basic conditions. This study indicates that wide ranging tests are required to fully understand the conditions under which patterned fibers will remain stable on surfaces.

It will also be desirable to characterize the surface properties of fibril-modified surfaces. The self-assembling amphiphilic EAK16-II fibers provide a good example of this type of characterization (Yang et al., 2007). Adsorption of fibers on a surface significantly changes the surface properties, including increasing the contact angle of water on mica and decreasing the contact angle of water on HPOG. This change in contact angle will subsequently change interactions between the surface with water, solvents, or biomolecules.

Larger micron-scale fiber patterns can be created on a surface by employing physical techniques in addition to surface templating. Several examples can be drawn from studies that employ nonamyloidogenic self-assembling protein systems. Hung recently described how the assembly of fibrous peptide amphiphiles can be directed using spatial confinement in micro-capillaries (Hung and Stupp, 2007). This method is a sonication-assisted solution embossing technique, where solvent evaporation drives assembly within a narrow channel. Sonication imparts energy to the system and improves alignment. Straight and curved patterns of aligned fibrils could be achieved using straight or curved channels cut by an electron beam as shown in Figure 6. The authors suggest that these techniques will be applicable to a wide range of other self-assembling systems.

In some cases, assembly can also be focused in the vertical direction away from the surface. This type of assembly can produce materials with very different properties from the same initial building blocks. Diphenylalanine-based peptides dissolved in 1,1,1,3,3,3-hexafluoro-2-propanol (HFP) solvent can be assembled vertically on a siliconized glass surface, as illustrated in Figure 7. The authors suggest that rapid solvent evaporation concentrates the peptide, generating a supersaturated solution that nucleates quickly on the surface (Reches and Gazit, 2006). The stacking of aromatic groups then leads to growth in the vertical direction. Electrostatic charges appear important to this growth and uncharged or negatively charged peptide analogs do not assemble vertically. Positively charged peptides do form highly orientated structures but only on negatively charged surfaces and not on positively charged surfaces, indicating that charge repulsion between the peptides and the surface stabilizes these structures. The specific interactions that mediate this assembly process suggest that it will be restricted to self-assembling systems containing aromatic motifs.

The studies highlighted in this section illustrate how surfaces can be used to direct the assembly of amyloid fibrils and other self-assembling

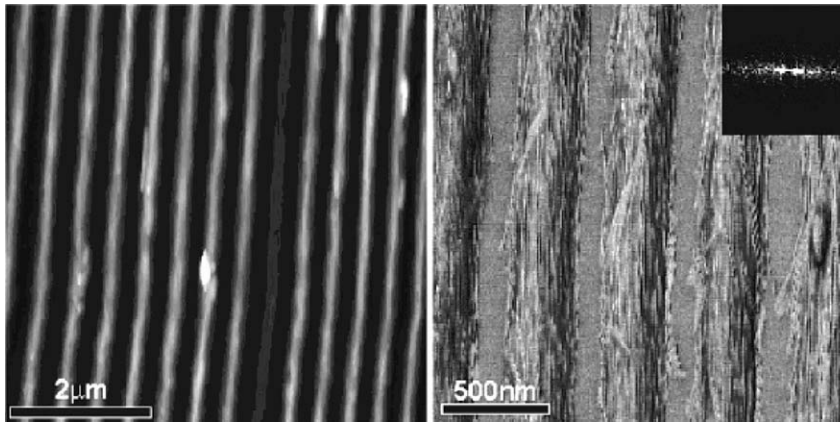


**Figure 6** Peptide amphiphile nanofibers that have been aligned during assembly using a sonication-assisted solution embossing technique. The images are atomic force microscopy height (left) and phase (right) images. The inset is a fast Fourier transform of the phase image showing the periodicity of the pattern. Reprinted with permission from Hung and Stupp (2007) (copyright 2007 American Chemical Society).

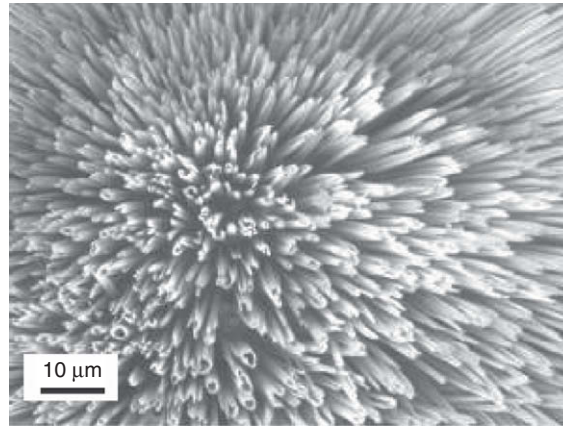


**Figure 7** Scanning electron microscopy image of vertically aligned diphenylalanine-based peptide nanotubes assembled on a glass surface. The scale bar is 10 μm in length. Reprinted by permission from Macmillan Publishers Ltd., *Nature Nanotechnology* (Reches and Gazit, 2006), copyright 2006 (http://www.nature.com/nnano/index.html).

systems. For further details on the ordered assembly of amphiphilic peptides at an interface and methods that can be used to characterize these assemblies, the reader is directed to a recent review by Rapaport (2006).

### 3.3. Surface interactions following assembly

The simplest way to coat a surface with fibrils following fibril assembly is to deposit a droplet of fibrils suspended in solution onto a surface. The individual fibrils will then sediment to the bottom of the droplet, make contact with the surface and adsorb. A large volume of solution can also be brought in contact with the surface. The strength of fibril binding will depend on the electrostatic, hydrophobic, or Van der Waals interactions between the fibrils and the surface. These interactions cannot necessarily be predicted from behavior observed during fibril assembly, as different regions of the polypeptide chain are likely to be involved in each case. Indeed, Losic observed that preformed Aβ fibrils preferred to adhere to hydrophobic surfaces, whereas Aβ peptides preferentially assembled at a hydrophilic step edge on HOPG (see Section 3.2 above; Losic et al., 2006). Similarly, fibrils constructed from different polypeptide sequences will display different behaviors at a surface, as the residues on the outside of the fibrils will differ between fibrils, and it is these residues that are likely to mediate fibril–surface interactions.

Following fibril deposition, the surface can be rinsed to remove any unbound fibrils and dried. Studies on model protein systems (Squires et al., 2006) suggest that drying does not change structural integrity of fibrils. A degree of natural alignment is observed for some fibrils deposited on a surface, as shown in Figure 8, although it is not yet understood how buffers and surface properties influence this alignment (Scheibel et al., 2003). The concentration of fibrils in solution and interactions between fibrils will certainly contribute to fibril alignment.

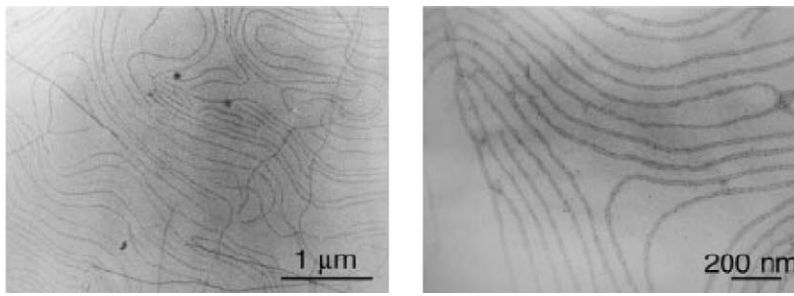


**Figure 8** Transmission electron microscopy image of fibrils formed from the Sup35 NM protein. The fibrils demonstrate natural alignment and are shown at low and high magnification on the left and right respectively (Scheibel et al., 2003). The scale bars are 1 µm and 200 nm in length, respectively (copyright © The National Academy of Sciences of the United States of America, all rights reserved, 2003).

For the majority of fibril systems, simple deposition results in layers of fibrils that are largely unordered. The thickness of the fibril layer can also vary. This section explores a variety of methods that can be used to induce fibrillar alignment on a surface or create surface patterns. It also details methods that can be used to induce covalent and noncovalent attachment of fibrils to the surface.

Electrostatic interactions between fibrils and a surface can be exploited to create micron-sized patterns of fibrils. Mesquida and colleagues (2005) used this approach to selectively deposit fibrils onto negatively charged stripes of mica that were exposed between alternating stripes of deposited cationic poly-L-lysine, as shown in Figure 9. The striped pattern was formed by directing poly-L-lysine through the channels of a polydimethysiloxane (PDMS) stamp that was placed in contact with the mica surface.

The fibril deposition observed by Mesquida is thought to be governed largely by electrostatics, and fibril binding could be switched from the negatively charged mica surface to the positively charged poly-L-lysine by raising the solution pH. This is presumably due to the ionization of exposed amino acid side chains on the fibril. This type of fibril behavior also suggests that salt may be used to screen electrostatic charges and prevent adhesion. Although this method does not create order within the patterns and the fibrils are orientated randomly, the method does effectively achieve micron-sized arrays of fibrils.

In a second study, Mesquida again exploited electrostatic interactions between fibrils and surfaces to create surface patterns. This second study employed AFM charge writing to position fibrils in lines several microns

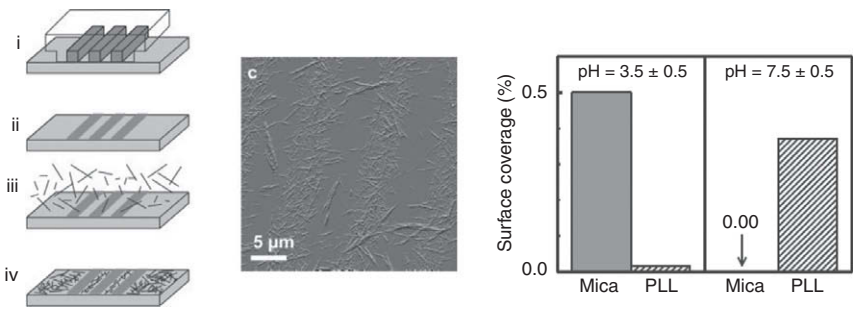


**Figure 9** Electrostatic patterning of pre-formed fibrils on a surface. Positively charged poly-L-lysine is patterned in stripes across a negatively charged mica surface using a PDMS stamp (left). Atomic Force Microscopy image showing how fibrils selectively deposit on the exposed mica surface at low pH (centre). The scale bar is 5 mm in length. Fibrils deposition can be switched from mica to poly-L-lysine as the solution pH is increased (right) (Mesquida, Ammann et al., 2005). Copyright Wiley-VCH Verlag GmbH & Co. KGaA. Reproduced with permission.

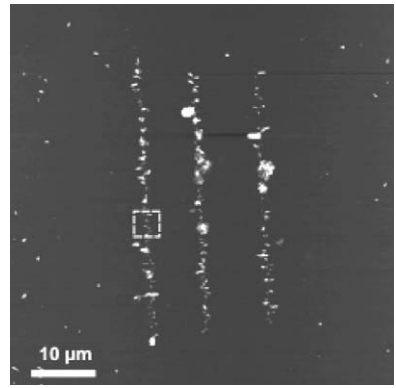


**Figure 10** Atomic force microscopy image of a fibril microarray. The pattern was created by charge-writing using atomic force microscopy. The scale bar is 10 µm in length. Reprinted with permission from Mesquida et al. (2006) (copyright 2006 American Chemical Society).

in length on a polymer surface, as shown in Figure 10 (Mesquida et al., 2006). The fibril cargo was suspended in water droplets within a water-in-perflurocarbon oil emulsion, generated by sonicating an aqueous solution of fibrils mixed with perflurocarbon. Three negatively charged lines were drawn on a polymethyl–methacrylate polymer surface using an AFM tip to which a small voltage was applied. The emulsion was then washed over this charged surface and fibrils deposited along the charge lines with an accuracy of 1–2 µm. Although the fibrillar structures did not form a continuous line and fibrils were not orientated along this line, fibril adsorption was specific to the charged areas. Once bound, the fibrils were also stable and were not removed from the surface by rinsing with water.

Molecular combing is another method that has been successfully employed to align individual amyloid fibrils on a surface (Herland et al., 2007). Molecular combing has been used extensively to align DNA molecules (Bensimon et al., 1994) and involves the movement of liquid along a surface. The receding air–liquid interface causes the alignment of partially adsorbed molecules largely due to viscous drag and surface tension. Herland and colleagues used this method to align insulin fibrils on glass. The authors stress the importance of achieving moderately strong interactions between the fibrils and the surface as this interaction facilitates alignment; if the interaction is too strong multiple parts of the fibril will adhere to the surface preventing alignment, if the interaction is too weak fibrils will not adsorb to the surface during combing preventing alignment. To overcome this problem, Herland incubated the fibril

droplet on the surface for 1 min prior to combing to ensure sufficient adsorption.

Herland found treated glass to be the most successful surface for molecular combing (Herland et al., 2007). This glass was rendered hydrophobic using a PDMS stamp or silanized with dichlorodimethylsilane (Herland et al., 2008). Following treatment, insulin fibrils that had been wrapped in the water-soluble polyelectrolyte poly(thiophene acetic acid) (PTAA) could be combed on the surface. In contrast, these fibrils did not adhere or align well on unmodified hydrophilic glass. Molecular combing could also be successfully applied to insulin fibrils coated with the water-insoluble conjugated polymer APFO-12 (Herland et al., 2008) demonstrating the wide applicability of this technique.

Another variation in molecular combing involves aligning fibrils directly on the surface of a PDMS stamp. These fibrils can then be print transferred onto a clean glass surface, as illustrated in Figure 11. Fibril layers printed in this way can withstand brief washing in water, oil, or ethanol solutions. Aligned fibrils may have scientific interest in addition to their potential as materials and Herland also used the aligned fibrils to help determine the orientation of the polymer chains, which are perpendicular to the fibril axis (Herland et al., 2008).

Magnetism is yet another successful method for the alignment of individual peptide fibers. Magnetite ($Fe_3O_4$) particles approximately 10 nm in size were noncovalently attached to diphenylanalanine nanotubes during fiber

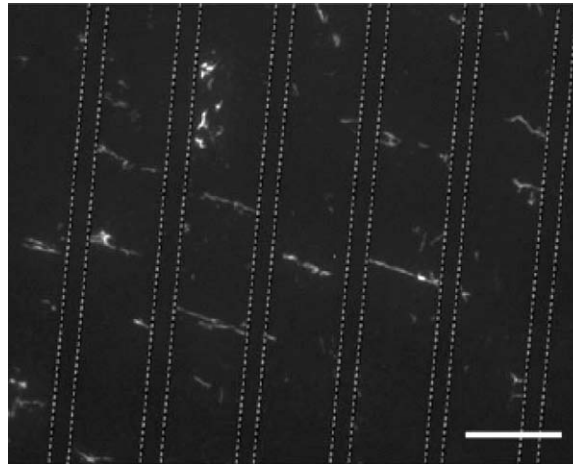

**Figure 11** Atomic Force Microscopy image of aligned PTAA coated insulin fibrils that have been transferred to a glass surface after molecular combing directly onto the surface of a PDMS stamp. The lines have been added to illustrate gaps within the PDMS stamp. The scale bar is 2 mm in length (Herland, Björk et al., 2007). Copyright Wiley-VCH Verlag GmbH & Co. KGaA. Reproduced with permission.

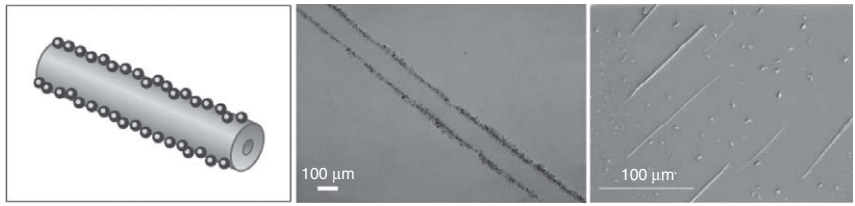


**Figure 12** Magnetically induced horizontal alignment of diphenylalanine-based peptide nanotubes. A noncovalent layer of magnetic nanoparticles coats the nanotubes during assembly (shown in the schematic left and transmission electron microscope image, middle). The application of an electric field induces alignment of the nanotubes suspended in ferrofluid (scanning electron microscopy image, right). The scale bars are 100 nm and 100 μm in length. Reprinted with permission from Macmillan Publishers Ltd., *Nature Nanotechnology* (Reches and Gazit, 2006), copyright 2006 (http://www.nature.com/nnano/index.html).

assembly, as shown in Figure 12. This attachment is thought to be mediated by hydrophobic interactions (Reches and Gazit, 2006). An external magnetic field of 0.5 T can then be used to induce alignment of fibers that have been suspended in a ferrofluid. In this case, a constant magnetic field was applied until the solution dried.

Larger patterned surfaces can also be achieved using inkjet printing. This technique has been used to create micron-sized letters of the alphabet containing diphenylalanine peptide nanotubes [tertbutoxycarbonyl–Phe–Phe–OH (Boc–Phe–Phe–OH)] on either transparent foil or indium–tin oxide (Adler-Abramovich and Gazit, 2008) as shown in Figure 13. This later

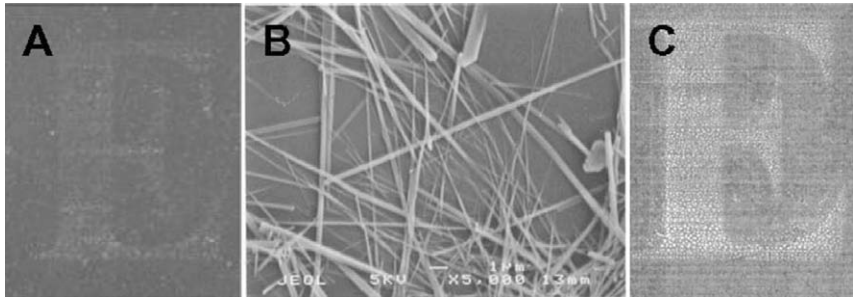


**Figure 13** Printed letters of the alphabet containing di-phenylalanine peptide nanotubes. A: single letter printed on transparent foil, B: detail of fibers within the letter shown in A. C: multiple printing of the same letter. All images were collected using Scanning Electron Microscopy. The scale bar in image B is 1 mm in length (Adler-Abramovich and Gazit, 2008). Copyright Blackwell publishing. Reproduced with permission.

surface may be useful for creating conducting materials. The morphology of the patterned fibers was dependent on the solvent used for printing. When the peptide was suspended in a mixture of hexafluorpropane and water, the printed peptides form fibers but when the peptide was suspended in hexafluorpropane and ethanol the letters contained only spheres. Although the fibers are not aligned within the printed features, the density of fibrils could be changed by increasing the peptide concentration or by printing multiple times on the same surface, and inkjet printing represents an effective technique for building larger structures from self-assembling peptides.

Covalent binding offers another way to immobilize amyloid fibrils on a surface and control fibril arrangement. Ha and Park (2005) covalently attached insulin fibrils to a *N*-hydroxysuccinimide-activated glass surface. The insulin fibrils were partially formed and they act as seeds which can further template the assembly of fibrils. By washing monomeric insulin over the surface, Ha and Park could form longer fibrils on the activated glass surface. This type of seeded assembly is different to both the surface-mediated assembly and surface-directed assembly described above (Sections 3.1 and 3.2, respectively). However, the surface may still influence fibril growth to the same extent as fibrils were observed to be thinner than those observed to form in solution. This method of covalent attachment has been used to screen factors that inhibit fibril formation, and it was an advance on previous studies which physically absorbed fibrils onto either glass or plastic in order to further template fibril growth (Esler et al., 1997, 1999).

Streptavidin–biotin interactions are another means of coupling fibrils to a surface, as shown in Figure 14. The binding between streptavidin–biotin is a noncovalent interaction that is remarkably strong and stable. Inoue and

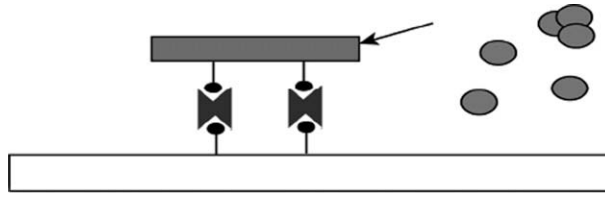

**Figure 14** Covalent attachment of fibrils to a surface. Sup35 fibrils were created from a mixture of Sup35 protein labelled with a Cy5-fluorescent tag, Sup35 labelled with biotin and unlabelled Sup35 protein. Labels were attached via a cystiene added to the C terminus of the Sup35 protein. The resulting fluorescent fibrils (shown in grey) were attached to a glass surface (shown in white) via biotin displayed on their surface, which linked to a further strepavidin-biotin anchor on the surface. Cy3-fluorescently labelled monomers (shown as circular species) were then be added to the solution to promote fibril extension (as indicated by the arrow). These experiments have been used to observe single fibril growth using total internal reflection fluorescence microscopy (Inoue and Kishimoto 2001).

colleagues (2001) formed fibrils from the Sup35 protein that had been labeled at the C terminal Cys residue with either a fluorphore or with biotin PEAC–maleimide. The resulting fibrils are fluorescent and display biotin on the fibril surface. These fibrils were then immobilized via a streptavidin linker to a biotinylated casein surface and monomer labeled with a second flurophore was added to observe fibril growth. One advantage of this technique is that unfixed fibrils can easily be washed away. Collins has also immobilized Sup35 fibrils via a biotin–streptavidin linker to a glass slide in order to observe individual fibril growth by TIRFM (Collins et al., 2004).

Dinca and colleagues (2008) have combined fibril self-assembly, lithographic features, and covalent and noncovalent binding to create three-dimensional patterned fibrillar structures that could be used in electronics or tissue engineering. Images of these structures, which are described as fibril bridges, are shown in Figure 15.

The positioning of fibrils between the lithographic columns was made specific through the use of both noncovalent and covalent chemistry shown in Figure 16. Dinca first deposited a layer of photobiotin on the column surface, this layer was then exposed to ultraviolet light in order to activate

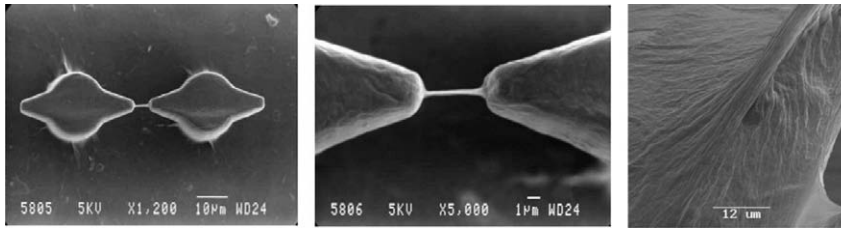


**Figure 15** Scanning electron microscopy images of lithographic columns and a fibril bridge that has formed between two of the columns (left). The fibril bridge and the point of fibril attachment to the column are shown at higher magnification (center and right respectively). The scale bars are 10 (left), 1 (center), and 12 µm (right) in length. Reprinted in part with permission from Dinca et al. (2008) (copyright 2008 American Chemical Society).

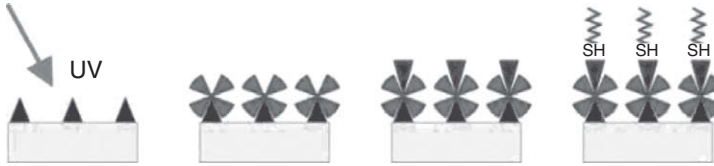


**Figure 16** Schematic illustrating the chemistry used to specifically immobilize peptides to lithographic features. Photobiotin (triangles) was activated with UV light to initiate binding. Biotin was next coupled to the surface (crosses), followed by the idoacetamide-functionalized biotin (triangles) and the final cysteine containing peptides. Reprinted with permission from Dinca et al. (2008) (copyright 2008 American Chemical Society).

protein binding to the column surface. Avidin was noncovalently bound to this layer, followed by idoacetamide-functionalized biotin. Fibrils displaying cysteine residues could then be covalently immobilized to the outer biotin layer via a SH–iodoacetamide reaction.

A suspension of preformed fibrils formed from a peptide containing cystiene was washed over the modified lithographic features and the fibril bridge initiated by drying. The fibril bridge contains an ensemble of fibrils that appear moderately aligned in Figure 15. No bridge was observed on columns without the required chemistry. This process of drying fibrils between pointed features has some analogies to the process used to form dried fibril stalks that are prepared for fiber X-ray diffraction. The formation of these site-specific fibril bridges could be widely applicable for the creation of nanoelectronic circuits and devices.

The studies outlined in this section show a number of different techniques that can be used to align fibrils and other peptide nanofibers in order to create micron-sized patterns from these self-assembling materials. This section also explored some of the covalent and noncovalent strategies for attaching fibrils to surfaces, and how these methods may be exploited to create three-dimensional patterns of fibrils that have an exciting range of potential applications.

## 4. APPLICATIONS

In this section, the potential application for amyloid fibrils and other self-assembling fibrous protein structures are outlined. These include potential uses in electronics and photonics presented in Section 4.1, uses as platforms for the immobilization of enzymes and biosensors presented in Section 4.2, and uses as biocompatible materials presented in Section 4.3. Each of these applications makes use of the ability of polypeptides to self-assemble and form nanostructured materials, a process that can occur under aqueous conditions. These applications also seek to exploit the favorable properties of fibrils such as strength and durability, the ability to arrange ligands on a nanoscale, and their potential biocompatibility arising from the natural materials used for assembly.

### 4.1. Electronics and photonics

The high order and aspect ratio of protein nanofibers and nanotubes makes these structures attractive candidates to construct nanowires. Consequently, amyloid fibrils and diphenylanalnine protein nanotubes are among a growing list of biomolecular templates being investigated for their ability to organize inorganic materials (Gazit, 2007). Both amyloid fibrils and peptide

nanotubes can withstand the harsh thermal and chemical conditions required for metal deposition and can be used to create wires up to several microns in length. Amyloid fibrils can also be constructed from a diverse range of peptide building blocks.

Wires have been made from amyloid fibrils using a modified version of amyloidogenic NM Sup 35 protein that displays cystiene residues along the fiber surface (Scheibel et al., 2003). Colloidal gold was covalently linked to these cystienes and the wires placed on gold electrodes where they were further coated with silver and gold layers by reductive deposition. Wires with diameters between 80 and 200 nm were produced, as shown in Figure 17. These wires demonstrate low resistance and conductive behavior ($R = 86\ \Omega$). In contrast, the uncoated fibers act as insulators and display no conductivity ($R > 10^{14}\ \Omega$). At higher voltages, the nanofibril wires also vaporize, effectively acting as fuses, illustrating the potential of these fibrils as wires for electrical circuits.

A different approach was taken by Reches and Gazit who exploited the hollow interior of diphenylalanine nanotubes to cast silver nanowires (Carny et al., 2006; Reches and Gazit, 2003). The peptide nanotubes were placed in a boiling ionic silver solution. Silver ions that had assembled inside the tube core were then reduced with citrate. The outer protein layer was next digested with the enzyme proteinase K, releasing the wire from its casing as shown in Figure 17.

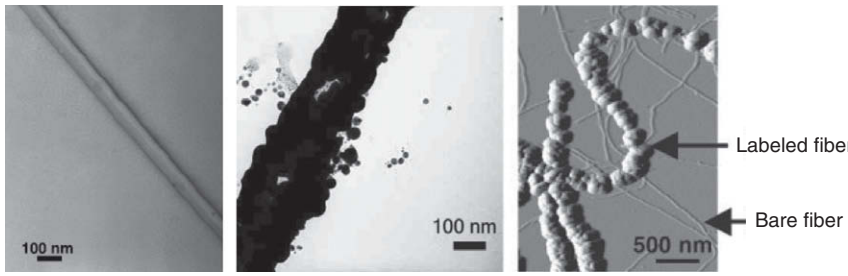


**Figure 17** A range of nanowires and nanotubes. Silver nanowires are cast inside diphenylananine nanotubes and the outer peptide layer digested with the enzyme Proteinase K (left), coaxial cables created from diphenylananine nanotubes containing silver and coated with gold (center) both imaged by transmission electron microscopy. Nanowires can also be constructed from the amyloidgenic protein NM Sup35 where layers of gold and silver coat the fiber as shown in the atomic force microscopy image (right). The scale bars are 100 nm (left and center) and 500 nm (right) in length. Left from Reches and Gazit (2003), reprinted with permission from AAAS. Centre reprinted in part with permission from Carny et al. (2006) (copyright 2006 American Chemical Society). Right from Scheibel et al. (2003) (copyright © The National Academy of Sciences of the United States of America, all rights reserved, 2003).

Coaxial fibers were also formed from diphenylalanine fibers (Carny et al., 2006). Coaxial fibers contain two metal layers separated by an insulating layer, in this case the peptide nanotube. Silver was again cast within the peptide nanotube but peptide linkers containing diphenylalanine and cystiene were also recruited to the outside of the tube where they interacted noncovalently with the surface. The cystiene residues were then used to attract gold nanoparticles before further reductive deposition of gold. This led to a gold-covered surface as shown in Figure 17. The conductive properties of these wires have not yet been tested, nevertheless Carny and colleagues suggest that the coaxial geometry will shield electromagnetic interference.

Remarkably, some peptide nanofibers can act as nanowires without the addition of a conductive metal layer. Fibers constructed from a polypeptide containing the sequence Val-Gly-Gly-Leu-Gly from the hydrophobic domain of elastin display an intrinsic blue-green fluorescence and have been found to be conductive (del Mercato et al., 2007). When cast onto gold electrodes by simple drop deposition and dried, these fibers conduct and display a high current. This conductivity is likely to be due to the water molecules that reside along the length of the fibril, as charge transport is highly dependent on humidity and does not occur in a vacuum. The authors suggest that charge transport and luminescent properties in these fibers are also related. Importantly, this study suggests that designed sequences can potentially be used as label-free nanowires.

Another approach toward fibrillar nanowires has been taken by Baldwin and colleagues (2006), who assembled a porphyrin binding protein onto the surface of an amyloid fibril. This binding protein could incorporate heme to form a functional b-type cytochrome. These fibrils could be developed to create wires for electron transfer, similar to structures observed in nature that consist of chains of heme molecules.

Conducting fiber cores have also been created from peptide amphiphiles that incorporate the hydrophobic conductive polymer poly(3,4-ethylenedioxythiophene) (PEDOT) into the fiber core (Tovar et al., 2007). The addition of ammonium persulfate to these structures triggers polymerization of the polymer resulting in a film of fibers that display high conductivity. The authors suggest that this approach is general and could be applied to sequester other conducting polymer precursors. The peptide amphiphiles containing these polymers may also find use as biosensors (see Section 4.2 below), if biological interactions with the fibers can be used to change the signal transferred along the conducting polymer. Peptide amphiphiles have also been created from peptides containing a diacetylene group within the alkyl tail that can be polymerized following assembly (Hsu et al., 2008), providing further scope for linking electronic properties to bioactivity.

Other inorganic materials have been assembled on a wide range of self-assembling protein structures. Many of these studies have sought to mimic nature, which can create a vast range of templated inorganic structures.

Copper has been immobilized on glycylglycine bolaamphiphile peptide nanotubes that display histidine residues, and paramagnetic gadolinium, a magnetic resonance image contrast agent, has been immobilized on nanofibers produced from peptide amphiphiles (see Gazit, 2007 and references therein).

Peptide amphiphiles have also been used to induce the nonorientated growth of cadmium sulfide nanocrystals and orientated the growth of hydroxyapatite along the fiber axis (Hartgerink et al., 2001; Sone and Stupp, 2004). The authors suggest these fibers could act as semiconductors (cadmium sulfate), could promote the mineralization of other components (cadmium sulfate), or could be used as biomaterials (hydroxyapatite; see section below). Silicon nanotubes have also been created by the condensation of tetraethoxysilane (TEOS) on β-sheet fibrils (Meegan et al., 2004) and peptide–amphiphile nanofiber templates (Yuwono and Hartgerink, 2007). This TEOS layer can then be calcified by heating, and the interior organic peptide template degraded, resulting in hollow silicon nanotubes.

Optoelectronics is another area where fibrils could be used. Herland and colleagues (2005) formed fibrils from a solution containing bovine insulin protein and one of two types of semi conducting conjugated oligoelectrolytes. Although it is not clear how the oligoelectrolytes are included within the fibril core, the ratios of each component, or the structure of the fiber core, the oligoelectrolytes appear to be arranged symmetrically and the fibrils form electrically active luminescent bundles. These wires demonstrate fluorescent quenching when a small voltage (0.9 V) is applied and quenching is reversed when the surrounding electrolytic solution is reduced by a second voltage (–0.3 V), suggesting that electric transfer occurs along the length of the fibril.

Preformed amyloid fibrils have also been coated with both water-soluble and water-insoluble conjugated polymers (Herland et al., 2007, 2008). The water-soluble conjugated polymer PTAA was found to align along the length of the fibril. The water-insoluble conjugated polymer, APFO-12, is an uncharged polar alternating polyfluorene derivative that was also found to form a highly ordered structure along the length of the fibril. Materials similar to APFO-12 have been used in solar cells and for light emitting diodes, where their order is essential to properties such as electrical transport. The authors suggest that such coated fibrils may prove useful as nanowires or in ordered films.

The polycylic fluorphore fluorene has also been assembled on the outside of fibrils constructed from the amyloidogenic TTR105-115 peptide (Channon et al., 2008). The fluroene unit has the ability to drive self-assembly. However, in this case the fluorene unit was attached to the TTR105-115 sequence which was used to drive fibril formation so that the fluorene unit was displayed on the fibril surface. Channon observed the transfer of

excitons from high energy absorbance sites to low-energy trapping sites along these fibrils, suggesting the fibrils could be used to construct light harvesting materials with properties analogous to those observed for photosynthesis in nature.

## 4.2. Platforms for enzyme immobilization and biosensors

An exciting potential use for protein fibers is as platforms for the immobilization of biologically active components, including enzymes or motor proteins (Gras, 2007; Karsai et al., 2008). These components can easily interface with protein nanofibers and could be linked to the protein unit prior to or following fiber assembly. In the case of amyloid fibrils, there are multiple sites where biomolecules could be attached. These include the polypeptide termini or amino acids that are typically exposed at multiple locations along the length of the fibril. The nanoscale order of amyloid fibrils can be used to control the position of biologically active elements, and immobilization can offer advantages such as enhanced enzymatic properties and stability. Moreover, multiple complementary components can be displayed on a single fibril, and this approach could be used to achieve sequential or cooperative biological processes.

Biosensors and devices may also include fiber components. Biosensors essentially contain two main components. These are the sensing element, which senses the molecule of interest, and the transducer, which generates a signal. Amyloid fibrils and other protein nanofibers could be used in biosensors in two ways. The first is as a scaffold to immobilize the sensing element on a nanoscale as described above. The second use is as a coating on the transducer where the presence of the protein fiber could enhance device performance. This enhancement could be carried out either with or without the aid of a further conductive coating (see Section 4.1 above).

The amyloidogenic Sup35 protein has been successfully used to immobilize three enzymes: barnase, carbonic anhydrase, and glutathione *S*-transferase (Baxa et al., 2002). Each of these enzymes was linked to the Sup35 sequence which drives assembly creating three different fusion proteins which successfully formed fibrils displaying functional enzymes on the fibril surface.

Artificial catalysts have also been incorporated into amphiphilic structures (Guler and Stupp, 2007). These catalysts were imidazolyl-functionalized peptides, which demonstrate a greater rate of 2,4-dinitrophenyl acetate hydrolysis when immobilized on the peptide amphiphile than the rate observed when the same enzyme is present in solution. Although the density of the enzymes on the fiber surface has not been established, the authors attribute the increase in enzymatic activity to the likely concentration of enzyme along the fiber surface, and this study illustrates one of the advantages of enzyme immobilization.

The hydrophobins are a case where protein nanofibers can play a dual role in creating a biosensor. They can aid in the immobilization of bioactive components within a biosensor and also add further functionality to the transducing element of a biosensor device. Hydrophobins are self-assembling β-sheet structures observed on the hyphae of filamentous fungi. They are surface active and aid the adhesion of hyphae to hydrophobic surfaces (Corvis et al., 2005). These properties can be used to create hydrophobin layers on glass electrodes. These layers can then facilitate the adsorption of two model enzymes: glucose oxidase (GOX) and hydrogen peroxidase (HRP) to the electrode surface. The hydrophobin layer also enhances the electrochemical properties of the electrodes.

Enzyme immobilization on a hydrophobin layer does not appear to significantly decrease enzyme properties, and these enzymes display similar substrate affinity to free enzymes. The specific activity of these enzymes may be lower than enzymes that are free in solution, but the immobilized enzymes also have the advantage of increased stability from 1 to 3 months (HRP and GOX, respectively).

The increased sensitivity of the electrodes coated with the hydrophobin layer is also appealing. The hydrophobin-modified electrodes allow $H_2O_2$, the product of glucose oxidation, to be detected at a concentration of 0.2 mM. This level is significantly lower than the detection limit of the bare electrode, which is 0.9 mM. The authors attribute the increase in electrode performance to the local accumulation of $H_2O_2$ at the electrode surface or a possible decrease in current in the presence of the hydrophobin layer.

Diphenylalanine nanotubes are a second example where self-assembling protein structures can have a dual role in biosensing. Yemini and colleagues (2005a) used diphenylalanine nanotubes to immobilize enzymes and to enhance the transducer component of the biosensor. In this case, the enzymes were linked to the preformed nanofibers by nonspecific chemical cross-linking using gluteraldehyde. The nanotubes were then covalently attached to a gold electrode via a thiol linkage. A further polyethyleneimine matrix was then deposited across the surface to capture and increase the concentration of reactive intermediates, enhancing sensor performance. This setup is shown in Figure 18.

The diphenylalanine nanotube sensors were based on the observation that peptide nanotubes improve the electrochemical properties of graphite and gold electrodes when deposited directly onto the electrode surface (Yemini et al., 2005b). The high surface area of the nanotubes and the potential alignment of aromatic residues are thought to contribute to the observed increase in conductivity. This property makes nanotube-coated electrodes and hydrophobin-coated electrodes suitable for use as amperometric biosensors that produce a current in response to an electrical potential across two electrodes.

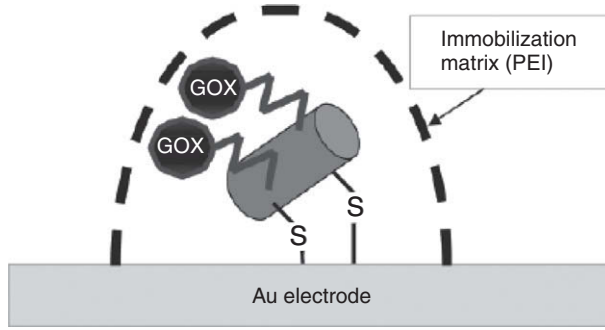


**Figure 18** Schematic of a glucose biosensor assembled from diphenylalanine peptide nanotubes. The enzyme GOX has been cross-linked to these nanotubes, which are further linked to the gold (Au) electrode and immobilized in a polyethyleneimine (PEI) matrix. The nanofibers act in two ways; they immobilize the sensing enzyme and enhance the transducer. Reprinted in part with permission from Yemini et al. (2005a) (copyright 2005 American Chemical Society).

Diphenylalanine nanotube sensors and hydrophobin sensors could be widely used for diabetic monitoring, food, and environmental sensing. For example, GOX and ethanol dehydrogenase were successfully immobilized on the surface of the diphenylalanine nanotube sensors (Yemini et al., 2005a). The presence of glucose resulted in the production of hydrogen peroxide by GOX and an increase in current across the electrodes. The presence of ethanol similarly resulted in the production of Nicotinamide adenine dinucleotide (NADH) by ethanol dehydrogenase and an increase in current across the electrodes. In both cases, the current generated by the nanotube sensors was greater than for uncoated sensors suggesting the potential utility of these devices.

Another biosensor for the sensitive detection of viruses is based on antibody functionalized peptide nanotubes (MacCuspie et al., 2008). Viral antibodies were immobilized on the end of peptide nanotubes formed from the bolaamphiphile peptide monomer, bis(*N*-a-amidoglycylglycine)-1,7-heptane dicarboxylate while flurophores were displayed on the side of the nanotubes. When the virus is mixed with these nanotubes, they aggregate leading to an increase in light scattering and fluorescence. This assay is highly sensitive and trace amounts ($10^3$ pfu/ml) of pathogens including herpes simplex virus type 2 (HSV-2), vaccinia, adenovirus, and influenza type B could be detected. This sensitivity is due to the high number of flurophores along the nanotube length which increase the sensitivity to $10^5$ times greater than traditional antibody–dye conjugates. This illustrates the broad potential of this nanofiber assay which could also utilize other self-assembling peptide systems.

The examples highlighted in this section illustrate the broad applicability of fibrils and other self-assembling systems as components in biosensors

and devices. These sensors may be applied to detect a host of biomolecular reactions or biomolecules. The model enzymes attached to these scaffolds also present proof of principle for the concept of enzyme immobilization on fibrils and other fibers.

## 4.3. Biocompatible materials

Self-assembling peptide systems may be developed as advanced materials for biomedical applications. These nanofibers can be used to study how cells respond to nanostructures; an important area which we are only beginning to understand. Protein fibers can also be designed to support cells and provide an environment that mimics natural tissue, providing the physical and chemical cues to promote particular cell behavior such as cell adhesion, cell migration, cell differentiation, or tissue regeneration. Structures that are shown to be biocompatible may also find roles as materials for in vitro and in vivo use. This could include applications as diverse as soft and hard tissue engineering, composites materials, coatings to increase device biocompatibility, and vehicles for drug delivery.

Functionalization is a central to many studies exploring the potential of polypeptide fibers as biocompatible materials, and fibers are often decorated with short bioactive tags that originate from the extracellular matrix (ECM). These tags can be displayed on protein fibers at much higher densities than that which occurs in nature and can also be displayed in unique and complimentary combinations.

There are two main ways to incorporate bioactive tags; the first is to include the sequence prior to assembly (see Sections 4.1 and 4.2 above for other examples). The second is to link the sequence following assembly either by covalent capture or by chemical cross-linking. Fibers that display these tags not only have typical dimensions of ECM proteins but can interact with cells in a similar way to the ECM.

A range of functionalized and unfunctionalized self-assembling fibrous structures have been tested for their biocompatibility and ability to provide cells with a favorable micro- and nanoenvironments for soft tissue engineering. In this section, studies that focus on amyloid fibrils, on peptide amphiphiles, on ionic complementary peptides, and on dipeptide structures are reviewed. Hard tissue engineering, composites, and coating are also explored followed by macroscopic structures and networks that can be created from fibrous protein structures.

### 4.3.1. Amyloid fibrils

Fibrils have broad potential for many of the bioapplications listed above. While some amyloid fibrils have negative associations with protein misfolding diseases, other fibrils demonstrate positive functions such as the fibrils that thought to occur in mammalian cells (Fowler et al., 2006); reviewed in

Section 2.1 above). These functional fibrils suggest that designed fibrils can be developed as compatible materials. Toxicology will be a potential issue for all structures that self-assemble on a nanoscale. However, the natural building blocks used to construct protein fibers may increase the biocompatibility of these structures compared to other man-made materials. Polypeptide self-assembly also represents a route for generating ECM-like structures that are not only simpler than their natural equivalents but also easier to prepare.

Recently, TTR1 fibrils have been decorated with the classic RGD tripeptide motif isolated from fibronectin, which encourages cell adhesion via integrin cell surface receptors (Gras et al., 2008). This bioactive tag was added to the TTR1 sequence which drives fibril assembly and the tag shown to be exposed on the fibril surface and accessible to cells following assembly. The RGD-modified fibrils were bioactive in a cell dissociation assay which measures the ability of fibrils to competitively bind to cells and induce cell detachment from a surface, as illustrated in Figure 19. In

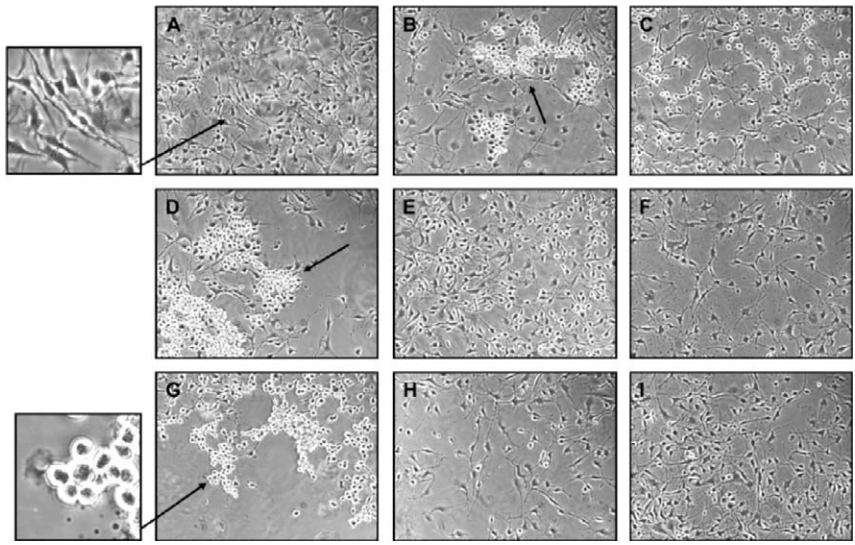


**Figure 19** Cell dissociation assay illustrating the bioactivity of RGD-modified fibrils. In this assay, a layer of 3T3 mouse fibroblast cells on tissue culture plastic (a) is exposed to a range of peptides and fibrils (b–i). Samples that are bioactive compete for cell binding and induce the dissociation of cells from the surface. The images show (b) after incubation with positive control RGDS peptide, (c) untreated cells following incubation, (d) after incubation with TTR–RGD1 peptide, (e) after incubation with TTR–RAD1 peptide, (f) after incubation with TTR1 peptide, (g) after incubation with TTR1–RGD fibrils, (h) after incubation with TTR1–RAD fibrils, and (i) after incubation with TTR fibrils. The arrows and enlarged image for (g) indicate clumps of dissociated cells. Reprinted from Gras et al. (2008) (copyright 2008, with permission from Elsevier).

contrast, an RAD control motif did not encourage cell interactions, nor did the base fibril structure. All three fibrils systems could also support non-specific cell attachment in a cell adhesion assay where cells were deposited on a surface coated with fibrils.

The density of the bioactive tags added to fibrous structures will determine the strength of binding, and the density of RGD tags on TTR1 fibrils was estimated to be as high as 2,000 RGD/μm equating to a distance of 0.5 nm between RGD tags (Gras et al., 2008). This density could be controlled by forming mixed fibrils from a solution containing TTR1–RGD doped with the plain TTR1 peptide. Using this method, RGD density could be reduced to as low as 12.8 RGD/μm (with 1% doping) equating to 85 nm between ligands. This range of RGD densities is biologically relevant as integrin receptors are typically spaced ~50 nm apart (Puleo and Bizios, 1991). Significantly, the cross-beta core of the fibril structure was also conserved suggesting that this method can be used to generate other combinations of fibril-forming peptides with a diverse range of bioactive tags.

The protein elastin presents another opportunity to create amyloid-like fibrils from natural proteins for the purpose of developing biomaterials. Elastin is found in tissue where it imparts elastic recoil, and fibrils formed from this protein may demonstrate some of the elastic properties of the constituent elastic proteins (Bochicchio et al., 2007). Elastin typically contains the sequence poly(ZaaGlyGlyYaaGly) (where Zaa, Yaa = Val or Leu) (Tamburro et al., 2005), and short stretches of the protein retain the ability to form structures similar to the original protein. Simple proline to glycine mutations in the hydrophobic domains of elastin can induce the formation of amyloid-like fibrils (Miao et al., 2003), suggesting that fibrillar materials can be easily generated from these sequences.

### 4.3.2. Peptide amphiphiles

Other polypeptide systems such as peptide amphiphiles show great promise as biocompatible materials for applications including tissue engineering. Peptide amphiphiles incorporating phosphoserine that are stabilized by four cysteine residues have been shown to induce mineralization, generating hydroxyapatite crystals aligned along the peptide amphiphile that resemble the natural structures found in bone (Hartgerink et al., 2001).

The ligand RGD has been incorporated into a range of peptide amphiphilic structures. This ligand was included in the self-assembling sequence used by Hartgerink (Hartgerink et al., 2001) and has been added to peptide amphiphiles following assembly using the activity of the enzyme tissue transglutaminase (Collier and Messersmith, 2003). RGD has also been shown to help induce the differentiation of mesenchymal stem cells and bone formation observed in the center of gels formed by peptide amphiphiles (Hosseinkhani et al., 2006c).

Complementary bioactive epitopes have since been displayed on peptide amphiphiles and used to support cells. These epitopes include RGD from fibronectin, or IKVAV and YIGSR from laminin which are thought to interact with neurons encouraging outgrowth and adhesion, respectively (Niece et al., 2003). The density of IKVAV can be as high as $7.1 \times 10^{14}$ epitopes per $cm^2$, which represents an increase of $10^3$ compared to the density of IKVAV naturally displayed in laminin (Silva et al., 2004). Murine neural progenitor cells were also encapsulated in these fibers, resulting in cell growth and rapid differentiation.

Synergistic sites have also been explored for display. Mardilovich displayed both RGD and the synergy site PHSRN (proline–histidine–serine–arginine) from fibronectin on the surface of a peptide amphiphile (Mardilovich et al., 2006). Importantly, the spacing and the ratio of hydrophobic to hydrophilic residues in the sequence between RGD and PHSRN was maintained in the new construct and cells adhered, spread and moved over the structures following assembly. The cells also deposited extracellular proteins indicating that the new construct performed as well as the original fibronectin protein.

Peptide branching has been used as a way to increase the density of ligand display and improve interactions with cells (Guler et al., 2006; Harrington et al., 2006). Harrington used a lysine dendron to improve the accessibility and number of ligands on the fiber surface, while Guler used orthogonal protecting group chemistry to introduce a branch at amine or lysine groups. Guler also introduced cyclic chemistry to improve the affinity between RGD and cell surface integrin receptors.

Branched peptide amphiphiles demonstrate superior properties when compared to their linear counterparts and enhance cell growth when coated on poly(glycolic acid) (PGA) tissue engineering scaffolds (Harrington et al., 2006). This finding suggests such materials may have potential in bladder tissue regeneration. Cells have also been shown to migrate through gels displaying very high densities of branched and linear RGD ligands (Storrie et al., 2007).

Blood vessels are another tissue engineering target where fibrous structures can be used to assist regeneration (Rajangam et al., 2008). Peptide amphiphiles containing a heparin binding consensus sequence have been used to bind to heparin and promote angiogenesis, these structures may also protect heparin from proteolytic cleavage in a biological environment. Fibroblast growth factor was also released from these fibers, effectively enhancing the growth of vessels in an angiogenesis assay.

These same peptide amphiphiles have been shown to assist mice to recover from spinal cord injuries (Tysseling-Mattiace et al., 2008). Both motor and sensory axons were able to cross the site of injury when peptide amphiphiles were injected and the peptide amphiphiles were stable in this in vivo environment for 1–2 weeks. Although recovery was only partial, this represents a remarkable achievement.

Gels formed from peptide amphiphiles mixed with basic fibroblast growth factor (bFGF) have also been used to successfully promote blood vessel formation in mice (Hosseinkhani et al., 2006a). Tabata and colleagues followed the release of bFGF, which is a chemo attractant that acts to promote the growth of fibroblast and endothelial capillary cells. bFGF release was prolonged and lasted for 750 h. The peptide amphiphiles were also degraded, although the rate was slow.

The fate of peptide amphiphiles will be critical to their development as materials for in vivo use. Studies by Beniash and colleagues found that cells entrapped within a network of peptide amphiphiles internalize fibers by endocytosis and store these fibers in the lysosome. In this case the fibers displayed a KGE motif, with similar charge properties to RGD, and the cells could proliferate within these scaffolds for at least 3 weeks. Studies of glucose and lactate concentrations suggest the cell may metabolize the peptide amphiphiles (Beniash et al., 2005), indicating that clearance of these peptides from the site of application is unlikely to be an issue for these structures.

Peptide amphiphiles may also be used for drug delivery. For example, Marini used fluorescently labeled peptide amphiphiles that were functionalized with the cyclo-RGD ligand and found that these structures were internalized by cells (Marini et al., 2002).

### 4.3.3. Ionic complementary peptides

Ionic complementary peptides have been extensively examined for biocompatibility in a series of short-term in vitro and in vivo assays. The majority, but not all, of these studies have focused on two model systems: RAD16 and EAK16.

RAD16 scaffolds have been shown to support the growth and differentiation of a number of cell types including a range of mammalian cells (Zhang et al., 1995). Neural cells attach and differentiate on RAD16 gels and growth is enhanced in the presence of neural growth factor (Holmes et al., 2000). RAD16 gels also provide a way to entrap migrating glial cells and neurons from hippocampal brain tissue sections, creating an effective way to recover these cells from a tissue section (Semino et al., 2004). Condrocytes have also been entrapped within a KLD-12 gel where they grow for 4 weeks, maintaining their morphology and depositing ECM rich in proteoglycans and collagen (Kisiday et al., 2002). This behavior suggests KLD-12 gels could be used to repair cartridge.

One of the most significant studies employing RAD16 gels was able to achieve axonal regrowth after damage to the optical nerve of a hamster (Ellis-Behnke et al., 2006). The RAD16-I peptide scaffold was injected into the wound area where it permitted significant regrowth allowing partial recovery of the optical nerve and return of some optical function for the animal.

Not all approaches to tissue engineering have been successful with RAD16 gels, suggesting that gels need to be tailored for particular applications. Davis and colleagues used RAD16 gels to create an environment appropriate for the culture of endothelial cells within heart tissue in vivo and found that endothelial cells invaded the gel and isolated cardio myocytes injected into the gel could survive (Davis et al., 2005). Gels were also found to be biocompatible and did not elicit an immune response. In contrast, Dubois found the RAD16-I gels with and without additional adhesion signals including YIG, RGD, and IKV did not support the survival of cells (Dubois et al., 2008). Inflammation was also observed and staining revealed the presence of inflammatory macrophage cells.

The primary sequence certainly has a significant effect on the interaction between nanofibers and cells. Sieminski illustrated this well by showing that human umbilical vein endothelial cells behaved differently on gels made from RAD16-I, RAD16-II, KF8, and KDL12 (Sieminski et al., 2008). The cells attached readily and formed microcapillary-like structures on RAD16-I and RAD 16-II but not the other gels, where cells remain rounded. Differences in protein adsorption to the fibers could not explain the differences in cell behavior, indicating that the chemistry of the primary sequence used to form the gel can determine cell interactions.

Genove and colleagues (2005) found that functionalized peptide nanofibers could effectively support human aortic endothelial cells. The N terminus of the RAD16 sequence was extended with two adhesion sequences from the ECM protein laminin and one from collagen: YIGSR, RYVVLPR, and TAGSCLRKFSTM, respectively. The new structures promote cell growth and improved cell function including the deposition of basement membrane. Competition assays with soluble peptides indicate that the cells do indeed recognize the adhesion sequences displayed on these fibers.

Other functional sequences have also been added to RAD16-I peptides to encourage bone growth (Horii et al., 2007). These sequences include osteogenic growth peptide ALK (ALKRQGRTLYGF) that is released following bone injuries, osteopontin cell adhesion motif DGR (DGRGDSVAYG) that regulates a number of cell functions, and a sequence containing RGD that is designed to promote adhesion called PGR (PRGDSGYRGDS). These new scaffolds enhanced osteoblast differentiation. Gels incorporating at least 70% of the PGR peptide also promoted cell migration to a depth of 300 μm within the scaffold. RAD16-I gels combined with a PolyHIPE polymer displaying hydroxyapetite have also shown high levels of osteoblast growth and mineralization, again suggesting the use of this gel for bone tissue engineering (Bokhari et al., 2005).

Another use for fibers formed from EAK16 and RAD16 peptides is as vehicles for drug delivery. EAK16 gels are able to effectively stabilize model

hydrophobic cargo such as the fluorphore pyrene (Keyes-Baig et al., 2004). The cargo can then be released into a simulated membrane made from phosophatidylcholine vesicles. Although this delivery mechanism is non-specific, this study suggests that ionic complementary peptides can be used to deliver compounds to the cell membrane.

The hydrophobic anticancer drug ellipticine is one of a number of other compounds that have been stabilized by association with fibrous proteins in aqueous solution (Fung et al., 2008 and references therein). Variants of EAK16 with different charge and hydrophobicity (EAK16II and EAK16-IV and EFK) were tested for their ability to stabilize the drug. The charge on the former two peptides enables these fibers to bind a protonated version of the drug, whereas the EFK can bind a neutral version of the drug using hydrophobic contacts. The bioactivity of these drugs was found to vary and this study illustrates that peptide properties will influence their behavior as drug carriers.

Nagai and colleagues (2006) have also examined the potential of gels formed from the peptide RAD16 to release drugs, and their study examined the diffusion of model compounds through the peptide amphiphile gel.

The properties of peptide fibers formed by ionic complementary peptides may need some tailoring to meet the different requirements for scaffolds and materials for drug delivery. However, these roles could be quite complementary. It is easy to envisage that mixtures of peptide fibers with different stabilities could be used to simultaneously stimulate and support the growth of soft tissues.

#### 4.3.4. Dipeptide nanotubes

Other research has focused on the interaction of cells with peptide structures that assemble via aromatic interactions. Cells have been grown on the surface of gels formed by Fluorenylmethoxycarbonyl (FMOC) modified diphenylalanine nanotubes (Mahler et al., 2006). Although cells were only grown for short time frames (24 h), the cells were viable on these scaffolds.

Similar work was performed by Jayawarna and colleagues. Chondrocytes were grown on a number of different hydrogels formed by FMOC-modified dipeptides and shown to grow for up to 10 days on these scaffolds (Jayawarna et al., 2007). In their earlier paper, Jayawarna also grew chondrocytes on top of hydrogels or incorporated cells within hydrogels formed by FMOC-dipeptides up to 7 days (Jayawarna et al., 2006).

#### 4.3.5. Hard tissue engineering, coatings, and other applications

Hard tissue engineering can include structures such as bone, and several examples of bone tissue engineering are presented in the sections above, other hard tissues that can potentially be repaired by self-assembling peptides include human dental enamel. Kirkhan and colleagues (2007) used self-assembling anionic peptides named $P_{11}$-4 to promote

remineralization in lesions in enamel. The observed effect was two fold; remineralization occurred at conditions of neutral pH and demineralization was inhibited at conditions of low pH. X-ray diffraction suggests these materials are capable of triggering hydroxyapetite formation without additional functional groups, suggesting this approach is suitable for the repair of enamel.

Other applications use self-assembling fibers to coat materials. For example, preassembled peptide amphiphiles have been covalently immobilized on titanium implant surfaces via a silane layer (Sargeant et al., 2008). Primary bovine artery endothelial cells or mouse calvarial preosteoblastic cells spread on these coated surface and proliferated to a far greater extent than on samples where the peptide amphiphiles had been drop cast onto the metal surface. This study therefore suggests that covalent attachment is required in order to prevent fibers lifting from the coated surface and to encourage maximal cell growth.

A further use for self-assembling peptides is as lubricants to reduce joint friction between cartilage surfaces (Bell et al., 2006). The amphiphilc peptide $P_{11}$-9 which resembles hyaluronic acid (HA), the natural lubricant in joints, successfully reduced joint friction in simulated experiments. Bell and colleagues suggest that this peptide may be a superior synthetic treatment compared to injection to replace HA, which is not suitable in all osteoarthritic cases.

Other applications for self-assembling fibrous structures not explored in depth here include applications as natural bioadhesives (Mostaert and Jarvis, 2007) or as components in membranes or other devices for filtration and bioseparation.

### 4.3.6. Macroscopic structures and networks

Many biomaterial applications require large macroscopic structures that can be easily handled. The ability of peptide fibrils and nanofibers to form larger ordered macroscopic structures will therefore be important to their use as biomaterials. Many self-assembling peptide systems do form gels and peptides such as EAK16 form membrane-like structures (Zhang et al., 1993). Other options for making larger structures include linking fibers to existing materials (see above) and forming composite materials.

There are a number of ways β-sheet structures can be altered so that they do form gels. One method is to link the chemical termini of peptides already incorporated into β-sheet fibers to form stiffer gels (Jung et al., 2008). Jung and colleagues used native chemical ligation (NCL), which links an N terminal cystiene to a C terminal thioester, to increase the storage modulus of gels formed by peptide amphiphiles. The resulting gels successfully induced the proliferation of primary human umbilical vein endothelial cells and when functionalized showed even higher levels of cell adhesion. The authors suggest that this approach can be

**Figure 20** Aerogels created from freeze-dried protein networks. Scanning electron microscopy images of aerogels made from protein gels (40 mg/ml) in water (left and center) and protein gels (40 mg/ml) in 95% water and 5% 1,1,1,3,3,3-hexafluoroisopropanol (HFIP). The inset on the left image shows the aerogel shape. The scale bars are 20 μm in length (left and center), 5 μm length (right), and 0.5 cm in length (inset) (Scanlon, Aggeli et al., 2007). Figure reproduced by kind permission of the IET and Scanlon, Aggeli et al. 2007.

used to modulate gel stiffness independently from peptide/fibrillar concentration.

The formation of porous aerogels is another way to make biomaterials from self-assembling peptide networks that are structured on a micron scale (Scanlon et al., 2007). Scaffolds are created by freezing the fibrous sample in liquid nitrogen. The ice is then sublimed in a vacuum. The resulting scaffolds have a micron-sized layered structure, as illustrated in Figure 20. Scanlon and colleagues suggest that the size and shape of the pores could be determined by controlling the rate and direction of freezing and ice crystal nucleation. The presence of solvents can also be used to influence the structure, as shown in Figure 20 (right). Freeze drying proved more reliable than supercritical fluid drying, possibly due to the complications of peptide solubility in liquid $CO_2$, and the freeze drying method could be applied to create similar structures from other protein nanofiber networks. The authors suggest that these aerogels could also find use as sensors or packing materials.

Peptide amphiphiles have also been incorporated within the interconnected pores of collagen sponges that were reinforced with polyglycolic acid (PGA) for mechanical strength, as illustrated in Figure 21 (Hosseinkhani et al., 2006b). These structures were shown to enhance the differentiation of osteogenic cells both in vitro and in vivo. In a second study, the peptide amphiphiles were mixed with growth factor bFGF prior to incorporation within the collagen sponges (Hosseinkhai et al., 2006a). The presence of the peptide amphiphiles made a significant difference to scaffold performance; the release profile of bFGF was sustained and bone formation was induced in scaffolds that had been implanted within a rat. Both these studies illustrate how macroscopic structures can be developed that successfully incorporate protein nanofibers.

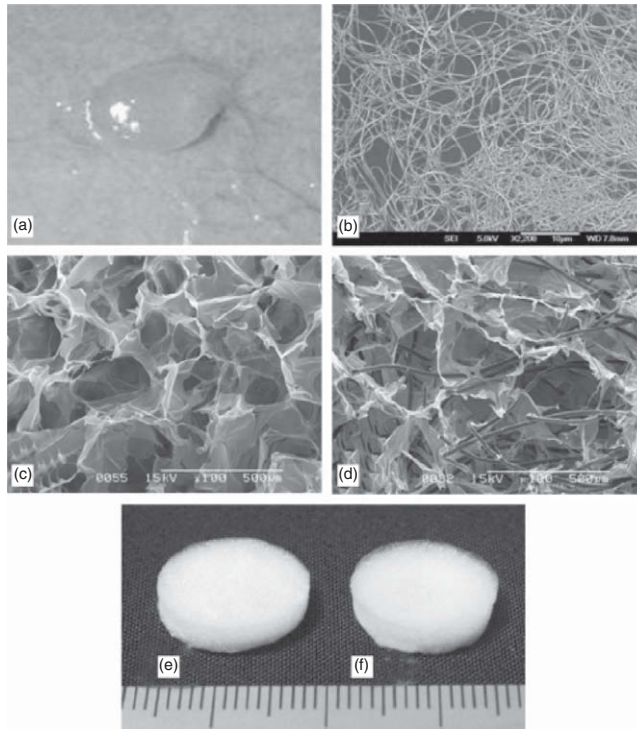


**Figure 21** Light microscopy image of a gel formed by adding culture media to a solution of peptide amphihiles (a), scanning electron microscopy image of the peptide amphiphilic structures (b), the collagen sponge without PGA fibers (c) and with PGA fibers (d) and light microscopy images of the sponges without (e) and with (f) the PGA fibers. Reprinted from Hosseinkhani et al. (2006b) (copyright 2006, with permission from Elsevier).

## 5. CONCLUSION

The discovery of different peptide sequences that can readily self-assemble to form protein fibers is significant as it provides a way to organize peptides and create fibrous structures on a nanoscale. Among these different systems, amyloid fibrils hold particular promise, as all polypeptides are thought to be capable of forming these resilient structures. Structures formed from self-assembling peptides are not only smaller than many man-made materials, they are also constructed from natural building blocks and can be tailored to display a range of useful properties. We already have extensive knowledge about how self-assembling systems organize in solution and on solid surfaces but there is an opportunity to extend this knowledge and exploit these interactions to form new structures and assemblies.

Polypeptide fibers are being rapidly developed as wires and structures for applications as diverse as enzyme immobilization, biosensing, and biomaterials. Larger macroscopic structures are also being developed from protein fibers. As our ability to manipulate these structures grows so too will the range of applications to which these fibers can be applied.

## REFERENCES

Adams, S., Higgins, A.M. et al. *Langmuir* **18**, 4854–4861 (2002).
Adler-Abramovich, L., and Gazit, E. *J. Pept. Sci.* **14**, 217–223 (2008).
Aggeli, A., Bell, M. et al. *Nature* **386**, 259–262 (1997).
Aggeli, A., Bell, M. et al. *J. Am. Chem. Soc.* **125**, 9619–9628 (2003).
Alexandrescu, A.T. *Protein Sci.* **14**, 1–12 (2005).
Allen, L.T., Fox, E.J. et al. *Proc. Natl. Acad. Sci. U.S.A.* **100**, 6331–6336 (2003).
Baldwin, A.J., Bader, R. et al. *J. Am. Chem. Soc.* **128**, 2162–2163 (2006).
Ban, T., Hoshino, M. et al. *J. Mol. Biol.* **344**, 757–767 (2004).
Baxa, U., Speransky, V. et al. *Proc. Natl. Acad. Sci. U.S.A.* **99**, 5253–5260 (2002).
Baxa, U., Taylor, K.L. et al. *J. Biol. Chem.* **278**, 43717–43727 (2003).
Bell, C.J., Carrick, L.M. et al. *J. Biomed. Mater. Res. A* **1**, 189–199 (2006).
Beniash, E., Hartgerink, J.D. et al. *Acta Biomater.* **1**, 387–397 (2005).
Bensimon, A., Simon, A. et al. *Science* **265**, 2096–2098 (1994).
Bochicchio, B., Pepe, A. et al. *Biomacromolecules* **8**, 3478–3486 (2007).
Bokhari, M.A., Akay, G. et al. *Biomaterials* **26**, 5198–5208 (2005).
Bosques, C.J., and Imperiali, B. *J. Am. Chem. Soc.* **125**, 7530–7531 (2003).
Bromley, E.H., Channon, K. et al. *ACS Chem. Biol.* **3**, 38–50 (2008).
Brown, C.L., Aksay, I.A. et al. *J. Am. Chem. Soc.* **124**, 6846–6848 (2002).
Bucciantini, M., Giannoni, E. et al. *Nature* **416**, 507–511 (2002).
Caflisch, A. *Curr. Opin. Chem. Biol.* **10**, 437–444 (2006).
Carny, O., Shalev, D.E. et al. *Nano Lett.* **6**, 1594–1597 (2006).
Carulla, N., Caddy, G.L. et al. *Nature* **436**, 554–558 (2005).
Channon, K., and Macphee, C.E. *Soft Matter* **4**, 647–652 (2008).
Channon, K.J., Devlin, G.L. et al. *J. Am. Chem. Soc.* **130**, 5487–5491 (2008).
Chapman, M.R., Robinson, L.S. et al. *Science* **295**, 851–855 (2002).
Claessen, D., Rink, R. et al. *Genes Dev.* **17**, 1714–1726 (2003).
Collier, J.H., and Messersmith, P.B. *Bioconjug Chem.* **14**, 748–755 (2003).
Collins, S.R., Douglass, A. et al. *PLoS Biol.* **2**, e321 (2004).
Colombo, G., Soto, P. et al. *Trends Biotechnol.* **25**, 211–218 (2007).
Corvis, Y., Walcarius, A. et al. *Anal Chem.* **77**, 1622–1630 (2005).
Davis, M.E., Motion, J.P. et al. *Circulation* **111**, 442–450 (2005).
del Mercato, L.L., Pompa, P.P. et al. *Proc. Natl. Acad. Sci. U.S.A.* **104**, 18019–18024 (2007).
Devlin, G.L., Knowles, T.P. et al. *J. Mol. Biol.* **360**, 497–509 (2006).
Dinca, V., Kasotakis, E. et al. *Nano Lett.* **8**, 538–543 (2008).
Dobson, C.M. *Trends Biochem. Sci.* **24**, 329–332 (1999).
Dos Santos, S., Chandravarkar, A. et al. *J. Am. Chem. Soc.* **127**, 11888–11889 (2005).
Dubois, G., Segers, V.F. et al. *J Biomed. Mater. Res. B Appl. Biomater.* **87B**, 1, 222–228 (2008).
Ellis-Behnke, R.G., Liang, Y.X. et al. *Proc. Natl. Acad. Sci. U.S.A.* **103**, 5054–5059 (2006).
Esler, W.P., Stimson, E.R. et al. *Nat. Biotechnol.* **15**, 258–263 (1997).
Esler, W.P., Stimson, E.R. et al. *Methods Enzymol.* **309**, 350–374 (1999).
Fandrich, M., Forge, V. et al. *Proc. Natl. Acad. Sci. U.S.A.* **100**, 15463–15468 (2003).
Fowler, D.M., Koulov, A.V. et al. *Public Library Sci. Biol.* **4**, 100–107 (2006).

Franks, G., and Meagher, L. *Colloids Surf. A* **214**, 99–110 (2003).
Fung, S.Y., Yang, H. et al. *PLoS One* **3**, e1956 (2008).
Gazit, E. *FEBS J.* **274**, 317–322 (2007).
Genove, E., Shen, C. et al. *Biomaterials* **26**, 3341–3351 (2005).
Ghadiri, M.R., Granja, J.R. et al. *Nature* **366**, 324–327 (1993).
Gras, S.L. *Aust. J. Chem.* **60**, 333–342 (2007).
Gras, S.L., Tickler, A.K. et al. *Biomaterials* **29**, 1553–1562 (2008).
Griffin, M.D., Mok, M.L. et al. *J. Mol. Biol.* **375**, 240–256 (2008).
Guijarro, J.I., Sunde, M. et al. *Proc. Natl. Acad. Sci. U.S.A.* **95**, 4224–4228 (1998).
Guler, M.O., Hsu, L. et al. *Biomacromolecules* **7**, 1855–1863 (2006).
Guler, M.O., and Stupp, S.I. *J. Am. Chem. Soc.* **129**, 12082–12083 (2007).
Ha, C., and Park, C.B. *Biotechnol. Bioeng.* **90**, 848–855 (2005).
Hamada, D., Yanagihara, I. et al. *Trends Biotechnol.* **22**, 93–97 (2004).
Harrington, D.A., Cheng, E.Y. et al. *J. Biomed. Mater. Res. A* **78**, 157–167 (2006).
Hartgerink, J.D., Beniash, E. et al. *Science* **294**, 1684–1688 (2001).
Herland, A., Bjork, P. et al. *Advan. Mater.* **17**, 1466–1471 (2005).
Herland, A., Björk, P. et al. *Small* **3**, 318–325 (2007).
Herland, A., Thomsson, D. et al. *J. Mater. Chem.* **18**, 126–132 (2008).
Holmes, T.C., de Lacalle, S. et al. *Proc. Natl. Acad. Sci. U.S.A.* **97**, 6728–6733 (2000).
Hong, Y., Legge, R.L. et al. *Biomacromolecules* **4**, 1433–1442 (2003).
Horii, A., Wang, X. et al. *PLoS One* **2**, e190 (2007).
Hortschansky, P., Schroeckh, V. et al. *Protein Sci.* **14**, 1753–1759 (2005).
Hosseinkhani, H., Hosseinkhani, M. et al. *Biomaterials* **27**, 5836–5844 (2006a).
Hosseinkhani, H., Hosseinkhani, M. et al. *Biomaterials* **27**, 5089–5098 (2006b).
Hosseinkhani, H., Hosseinkhani, M. et al. *Biomaterials* **27**, 4079–4086 (2006c).
Hosseinkhai, H., Hosseinkhani, M. et al. *Tissue Eng.* **13**, 11 (2007).
Hoyer, W., Cherny, D. et al. *J Mol Biol* **340**, 127–139 (2004).
Hsu, L., Cvetanovich, G.L. et al. *J. Am. Chem. Soc.* **130**, 3892–3899 (2008).
Hung, A.M., and Stupp, S.I. *Nano Lett.* **7**, 1165–1171 (2007).
Inoue, Y., Kishimoto, A. et al. *J. Biol. Chem.* **276**, 35227–35230 (2001).
Jayawarna, V., Ali, M. et al. *Advan. Mater.* **18**, 611–614 (2006).
Jayawarna, V., Smith, A. et al. *Biochem. Soc. Trans.* **35**, 535–537 (2007).
Jung, J.P., Jones, J.L. et al. *Biomaterials* **29**, 2143–2151 (2008).
Kammerer, R.A., and Steinmetz, M.O. *J. Struct. Biol.* **155**, 146–153 (2006).
Karsai, A., Grama, L. et al. *Nanotechnology* **34**, 345102/1–7 (2007).
Karsai, A., Murvai, U. et al. *Eur. Biophys. J.*, 1133–1137 (2008).
Kellermayer, M.S.Z., Karsai, A. et al. *Proc. Natl. Acad. Sci. U.S.A.* **105**, 141–144 (2008).
Keyes-Baig, C., Duhamel, J. et al. *J. Am. Chem. Soc.* **126**, 7522–7532 (2004).
Kirkham, J., Firth, A. et al. *J. Dental Res.* **86**, 426–430 (2007).
Kisiday, J., Jin, M. et al. *Proc. Natl. Acad. Sci. U.S.A.* **99**, 9996–10001 (2002).
Knowles, T.P., Shu, W. et al. *Proc. Natl. Acad. Sci. U.S.A.* **104**, 10016–10021 (2007).
Kowalewski, T., and Holtzman, D.M. *Proc. Natl. Acad. Sci. U.S.A.* **96**, 3688–3693 (1999).
Krebs, M.R., Bromley, E.H. et al. *J. Struct. Biol.* **149**, 30–37 (2005).
Krebs, M.R., Morozova-Roche, L.A. et al. *Protein Sci.* **13**, 1933–1938 (2004).
Linse, S., Cabaleiro-Lago, C. et al. *Proc. Natl. Acad. Sci. U.S.A.* **104**, 8691–8696 (2007).
Losic, D., Martin, L.L. et al. *Biopolymers* **84**, 519–526 (2006).
Lowik, D.W., Meijer, J.T. et al. *J. Pept. Sci.* **14**, 127–133 (2008).
MacCuspie, R.I., Banerjee, I.A. et al. *Soft Matter* **4**, 833–839 (2008).
MacPhee, C.E., and Dobson, C.M. *J. Mol. Biol.* **297**, 1203–1215 (2000a).
MacPhee, C.E., and Dobson, C.M. *J. Am. Chem. Soc.* **122**, 12707–12713 (2000b).
MacPhee, C.E., and Woolfson, D.N. *Curr. Opin. Solid State Mater. Sci.* **8**, 141–149 (2004).
Mahler, A., Reches, M. et al. *Advan. Mater.* **18**, 1365–1370 (2006).

Mardilovich, A., Craig, J.A. et al. *Langmuir* **22**, 3259–3264 (2006).
Marini, D.M., Hwang, W. et al. *Nanoletters* **2**, 295–299 (2002).
Meegan, J.E., Aggeli, A. et al. *Advan. Funct. Mater.* **14**, 31–37 (2004).
Meersman, F., and Dobson, C.M. *Biochim. Biophys. Acta* **1764**, 452–460 (2006).
Mesquida, P., Ammann, D.L. et al. *Advan. Mater.* **17**, 893–897 (2005).
Mesquida, P., Blanco, E.M. et al. *Langmuir* **22**, 9089–9091 (2006).
Miao, M., Bellingham, C.M. et al. *J. Biol. Chem.* **278**, 48553–48562 (2003).
Mimna, R., Camus, M.S. et al. *Angew. Chem. Int. Ed. Engl.* **46**, 2681–2684 (2007).
Mostaert, A.S., and Jarvis, S.P. *Nanotechnology* **18**, 044010 (2007).
Mucke, L., Masliah, E. et al. *J. Neurosci.* **20**, 4050–4058 (2000).
Nagai, Y., Unsworth, L.D. et al. *J. Control Release* **115**, 18–25 (2006).
Nayak, A., Dutta, A.K. et al. *Biochem. Biophys. Res. Commun.* **369**, 303–307 (2008).
Narrainen, A.P., Hutchings, L.R., *Soft Matter* **2**, 126–128 (2006).
Niece, K.L., Hartgerink, J.D. et al. *J. Am. Chem. Soc.* **125**, 7146–7147 (2003).
Nielsen, L., Khurana, R. et al. *Biochemistry* **40**, 6036–6046 (2001).
Nilsson, M.R. *Methods* **34**, 151–160 (2004).
Pauling, L., and Corey, R.B. *Proc. Natl. Acad. Sci. U.S.A.* **37**, 251–256 (1951).
Pearce, F.G., Mackintosh, S.H. et al. *J. Agric. Food Chem.* **55**, 318–322 (2007).
Puleo, D.A., and Bizios, R. *Bone* **12**, 271–276 (1991).
Rajangam, K., Arnold, M.S. et al. *Biomaterials* **29**, 3298–3305 (2008).
Rapaport, H. *Supramol. Chem.* **18**, 445–454 (2006).
Reches, M., and Gazit, E. *Science* **300**, 625–627 (2003).
Reches, M., and Gazit, E. *Nat. Nanotechnol.* **1**, 195–200 (2006).
Relini, A., Canale, C. et al. *J. Biol. Chem.* **281**, 16521–16529 (2006).
Rocha, S., Krastev, R. et al. *Chem. Phys. Chem.* **6**, 2527–2534 (2005).
Sargeant, T.D., Rao, M.S. et al. *Biomaterials* **29**, 1085–1098 (2008).
Scanlon, S., Aggeli, A. et al. *Micro. Nano Lett.* **2**, 24–29 (2007).
Scheibel, T., Kowal, A.S. et al. *Curr. Biol.* **11**, 366–369 (2001).
Scheibel, T., Parthasarathy, R. et al. *Proc. Natl. Acad. Sci. U.S.A.* **100**, 4527–4532 (2003).
Semino, C.E., Kasahara, J. et al. *Tissue Eng.* **10**, 643–655 (2004).
Sharp, J.S., Forrest, J.A. et al. *Biochemistry* **41**, 15810–15819 (2002).
Sieminski, A.L., Semino, C.E. et al. *J. Biomed. Mater. Res. A* **87A**, 2, 494–504 (2008).
Silva, G.A., Czeisler, C. et al. *Science* **303**, 1352–1355 (2004).
Smith, J.F., Knowles, T.P. et al. *Proc. Natl. Acad. Sci. U.S.A.* **103**, 15806–15811 (2006).
Smith, M.I., Sharp, J.S. et al. *Biophys. J.* **93**, 2143–2451 (2007).
Sohma, Y., Hayashi, Y. et al. *Biopolymers* **76**, 344–356 (2004).
Sone, E.D., and Stupp, S.I. *J. Am. Chem. Soc.* **126**, 12756–12757 (2004).
Squires, A.M., Devlin, G.L. et al. *J. Am. Chem. Soc.* **128**, 11738–11739 (2006).
Stefani, M. *Neuroscientist* **13**, 519–531 (2007).
Stevens, M.M., and George, J.H. *Science* **310**, 1135–1138 (2005).
Storrie, H., Guler, M.O. et al. *Biomaterials* **28**, 4608–4618 (2007).
Sunde, M., Serpell, L.C. et al. *J. Mol. Biol.* **273**, 729–739 (1997).
Talbot, N.J. *Curr. Biol.* **13**, R696–R698 (2003).
Tamburro, A.M., Pepe, A. et al. *J. Biol. Chem.* **280**, 2682–2690 (2005).
Taniguchi, A., Sohma, Y. et al. *J. Am. Chem. Soc.* **128**, 696–697 (2006).
Tovar, J.D., Rabatic, B.M. et al. *Small* **3**, 2024–2028 (2007).
Tuchscherer, G., Chandravarkar, A. et al. *Biopolymers* **88**, 239–252 (2007).
Tysseling-Mattiace, V.M., Sahni, V. et al. *J. Neurosci.* **28**, 3814–3823 (2008).
Waterhouse, S.H., and Gerrard, J.A. *Aust. J. Chem.* **57**, 519–523 (2004).
Westermark, P., Benson, M.D. et al. *Amyloid* **12**, 1–4 (2005).
Whitehouse, C., Fang, J. et al. *Angew. Chem. Int. Ed. Engl.* **44**, 1965–1968 (2005).
Woolfson, D.N., and Ryadnov, M.G. *Curr. Opin. Chem. Biol.* **10**, 559–567 (2006).

Wright, C.F., Teichmann, S.A. et al. *Nature* **438**, 878–881 (2005).
Yang, H., Fung, S.Y. et al. *PLoS One* **2**, e1325 (2007).
Yemini, M., Reches, M. et al. *Anal. Chem.* **77**, 5155–5159 (2005a).
Yemini, M., Reches, M. et al. *Nano Lett.* **5**, 183–186 (2005b).
Yuwono, V.M., and Hartgerink, J.D. *Langmuir* **23**, 5033–5038 (2007).
Zhang, F., Du, H.-N. et al. *Angew. Chem. Int. Ed.* **45**, 3611–3613 (2006).
Zhang, S., Holmes, T. et al. *Proc. Natl. Acad. Sci. U.S.A.* **90**, 3334–3338 (1993).
Zhang, S., Holmes, T.C. et al. *Biomaterials* **16**, 1385–1393 (1995).
Zhu, M., Souillac, P.O. et al. *J. Biol. Chem.* **277**, 50914–50922 (2002).
Zurdo, J., Guijarro, J.I. et al. *J. Am. Chem. Soc.* **123**, 8141–8142 (2001).